EFFECT OF BIO-CEMENTATION

ON THERMAL PROPERTIES OF

SILTY SAND

by

Pinar Gunyol

A thesis submitted in partial fulfillment
of the requirements for the degree

of

Master of Science

in

Civil Engineering

MONTANA STATE UNIVERSITY
Bozeman, Montana

May 2022

DEDICATION

I dedicate this thesis to my family and friends for their unconditional love and support, and to all researchers who believe in building a sustainable future.

ACKNOWLEDGEMENTS

I would like to thank my advisors, Dr. Mohammad Khosravi, Dr. Adrienne Phillips and Dr. Kathryn Plymesser for their motivation and guidance throughout my graduate studies. I am thankful to have had Dr. Joel Cahoon as my undergraduate advisor who encouraged me to pursue my Master’s degree.

Thanks to Air Force Research Laboratories and the Montana Department of Transportation who provided my funding. Special thanks to members of Center for Biofilm Engineering for their assistance and constant support; Micah Coburn for the extensive training on biochemical testing and taking great microscopy images, Al Parker for his assistance in the statistical analysis, Joe Eldring for his help with the design process, Hudson Dorian for his assistance on soil testing, Taha Alper Şen for his help and company in the lab, and Arda Akyel for his guidance throughout my studies in the Bioprocess Lab and support during difficult times.

TABLE OF CONTENTS

TABLE OF CONTENTS CONTINUED

LIST OF TABLES

LIST OF FIGURES

Figure Page

LIST OF FIGURES CONTINUED

ABSTRACT

In recent years, there has been an increasing interest in the use of biological technologies in geotechnical engineering to improve thermal properties of geomaterials. Urea hydrolysis is a chemical reaction which can generate favorable conditions that result in the precipitation of calcium carbonate. Certain microbes or plant sources produce the urease enzyme which catalyzes the hydrolysis of urea to form carbonate ($CaCO_3$) to bond soil particles. Cementation located between the grain particles acts as a highly conductive heat transfer path by increasing the contact area between the sand particles. In this thesis, the applicability of bio-cementation via microbially induced calcite precipitation (MICP) on silty sand specimens with different fines contents of 0%, 5%, and 15% were investigated. MICP promoting fluids were injected into sand-filled columns and the resulting calcium conversion was measured. At the end of the injections, the MICP treated specimens were tested for cementation uniformity. The amount of precipitated $CaCO_3$ gradually decreased as the distance from the injection ports increases. The observed bio-cementation distribution could be attributed to the filtration of bacterial cells through the soil particles. The resulting effect of filtration on $CaCO_3$ distribution was observed to be more prominent for silty sands, presumably due to the presence of fine grains. Thermal conductivity measurements were assessed after each pulse during the MICP treatment using a TR-3 sensor. Under the saturated and untreated conditions, thermal conductivity increased with increasing fines content. In addition, MICP treatment can increase the thermal conductivity of saturated silty sands with the increasing number of treatment pulses. An increase of about 18% in thermal conductivity of the soil was achieved at an average $CaCO_3$ content of 10.7% presumably due to the formation of calcium carbonate bridges binding the soil grains together. The results presented herein suggests that MICP treatment can be a viable option to increase the thermal conductivity of soils in the range of fines content studied here (less than 15%). The findings of this research could be used to improve the efficiency of geothermal boreholes and other energy geo-structures using MICP by improving thermal conductivity of dry and partially saturated soil.

CHAPTER ONE

INTRODUCTION

Background

Geothermal energy is a renewable, and sustainable energy resource, that has various engineering applications, such as ground source heat pumps (GSHPs) and geothermal energy piles (GEPs). The application of Geothermal Energy as a renewable heat source is well developed around the world due to its environmental advantages and long-term economic benefit (Sinyak, 1994). Geothermal heat can be extracted from shallow or deep layers of earth through thermo-active foundations or boreholes based on mechanisms of heat transfer, including convection, conduction, and radiation. Typical underground locations in which thermal energy is stored are: 1) aquifers, which are mostly considered for open-loop systems, 2) boreholes, and 3) rock caverns or pits (McCartney et al., 2016). The efficiency of underground energy structures is affected by the geothermal properties of soil such as thermal conductivity, thermal diffusivity, and ground temperature. The thermal conductivity of the subsurface is a key parameter in the design of geothermal systems (Pouloupatis et al., 2017), as heat transfer in soil can be improved by increasing thermal conductivity. Interest in the use of biological technologies in geotechnical engineering to improve soil properties has been rising in recent years (Gomez et al., 2017; Martinez et al., 2020; Montoya & DeJong, 2015a).

Heat Transfer Mechanism in Soil

Heat transfer in soil consists primarily of three mechanisms: 1) conduction, 2) convection, and 3) radiation. Other mechanisms that are of high importance to heat transfer in soil include: 4) vaporization and condensation, 5) freezing and thawing, and 6) ion exchange (Brandl, 2006). Figure 1.1 shows the main mechanisms of heat transfer through the soil. The preferred path for heat to transfer through soils is through the solid particles.

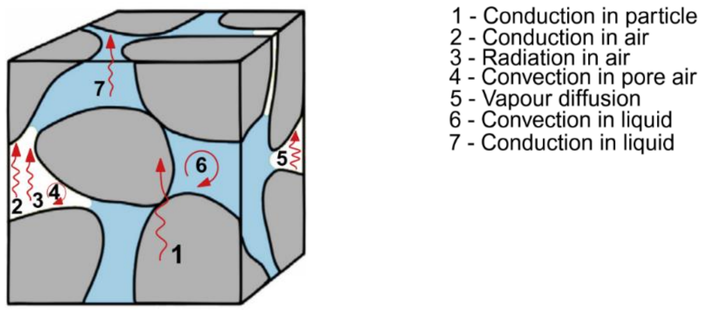

Figure 1.1. Heat transfer paths in soil (Alrtimi et al., 2016)

Heat transfer by conduction, which is the predominant heat flow mechanism in soil, refers to the flow of heat within solids and fluids (Dawoud et al., 2007). In the convection heat transfer mechanism, heat transfer occurs through the convection of a fluid and the fluid's motion (Brandl, 2006). Heat transfer by convection can occur by either natural or forced flow. In natural convection, the heat largely transfers due to the migration of air and/or water molecules in the soil, which occurs by a difference in density due to temperature change. Forced convection occurs by any external means (i.e., groundwater flow). Heat transfer by convection is usually negligible in soils with grain sizes smaller than sand (Farouki, 1981). Heat propagation through radiation occurs in soil pore spaces due to the motion of electromagnetic waves or alternatively by photons. Heat transfer in soil by radiation is usually negligible, comprising less than 2% of heat transfer in natural soil (Rees et al., 2000) and up to 10% of total heat transfer in coarse aggregates (Farouki, 1981).

Heat transfer in soil varies with grain size, density, and water content of the soil layer. Grain size influences other soil parameters such as porosity, permeability, and specific surface area, which are the primary factors affecting soil's thermal conductivity. Therefore, grain size is a secondary parameter that should be considered when evaluating the primary parameters (Midttømme & Roaldset, 1998). Other important structural factor influencing the thermal properties of soil is the number and nature of the contacts between soil particles.

Effect of Bio-Cementation on Thermal Properties of Soil

Microbes can alter the surrounding chemical environment to induce the precipitation of calcium carbonate ($CaCO_3$), a form of bio-cement (DeJong et al., 2010; Phillips et al., 2013; van Paassen et al., 2010). One mechanism that has been researched extensively is the microbe or plant produced enzyme urease, which promotes the hydrolysis of urea to change saturation conditions, which in the presence of calcium results in the precipitation of calcium carbonate (Cuthbert et al., 2013; Ebigbo et al., 2012b; Hommel et al., 2015; Mitchell et al., 2013; Phillips et al., 2016; Phillips et al., 2013). In the presence of urea, the urease enzyme catalyzes the hydrolysis of urea, altering the chemical environment towards favorable saturation conditions for the precipitation of $CaCO_3$ in the presence of calcium (Equation 1.1).

$$(NH_2)_2CO + 2H_2O + Ca^{2+} \rightarrow 2NH_4^+ + CaCO_3 \quad (1.1)$$

In this process, the precipitation of $CaCO_3$, often in the stable mineral form calcite, can serve to bind together porous media including soil matrices. Bio-cemented sand treated by MICP has been shown to be effective in reducing soil settlement (DeJong et al., 2006; van Paassen et al., 2010), increasing soil shear strength (Chou et al., 2011b; DeJong et al., 2006; Ismail et al., 2002a), and improving soil stiffness (Feng & Montoya, 2015; Lin et al., 2016b; Montoya & DeJong, 2015a).

The MICP treatment primarily affects the average dry density. Changes in thermal conductivity values are expected to reflect changes in dry density changes with bio-cementation level. Precipitation of calcite results in an increase in the solids content and therefore, the average dry density of the soil through the process of binding particles together at their contacts by calcite bridges (Whiffin et al., 2007). The surface area of interparticle contacts and contacts per unit volume are important parameters that determine thermal conductivity in dry soils. The precipitation of calcite results in an increase in the solids content, through the process of binding particles together at their contacts by calcite bridges. To increase the contact areas between soil particles, the microbially induced calcite precipitation (MICP) technique can be utilized to enhance the thermal properties of soil.

The medium present in the pore voids can affect the efficiency of heat transfer between the particles. Replacing the air in the pore voids with water results in increased heat transfer between the soil particles. Martinez et al. (2019) showed that the thermal conductivity of a dry soil specimen with 0% saturation, was increased by 860% when the specimen became fully saturated. The effect of water content on the thermal conductivity is more significant at lower degrees of saturation. The increase in thermal conductivity decelerates with an increase in the degree of saturation for both MICP treated and untreated soils (Venuleo et al., 2016). At higher levels of saturation (i.e., capillary and funicular regimes), particle contacts and presence of water are the governing factors for the increased heat transfer, and small volumes of air have a comparatively insignificant effect on the thermal conductivity of the soil (Likos, 2015).

Cementation sites between the grain particles can act as conductive heat transfer paths by increasing the contact area among sand particles, since the thermal conductivity of calcite ($k_{calcite}$ ~5 W/m.K) is much higher than air (k_{air} ~ 0.03 W/m.K). Precipitation of calcium carbonate results in an increase in the solids content and therefore, the average dry density of the soil (Whiffin et al., 2007). As the cementation in the soil matrix increases, calcite crystals formed between soil particles decreases porosity and increase number of particle contacts.

The surface area of the contact points between the particles significantly increases with calcite crystals formed between the grain particles. Even with a small amount of calcite mass, heat flow is more efficient between cemented grain particles leading to a reduction of the interparticle thermal resistivity. Recent studies have shown that precipitation of calcium carbonate through MICP process can increase the thermal conductivity of sands by up to 300% (Martinez et al., 2019; Venuleo et al., 2016).

Previous studies on the effect of bio-cementation on soil behavior have mainly focused on thermal properties of medium sand (e.g., median size of 0.2 mm). However, the thermal behavior of bio-cemented soil as a function of the amount of $CaCO_3$ formed and fines content require further investigation. Presence of fine-grained soil (e.g., silt) in the soil matrix adds complexity to applicability of MICP technique to enhance thermal properties of soil due to smaller pore sizes and larger specific surface areas (Zamani & Montoya, 2018). Midttømme and Roaldset (1998) reported that grain size distribution is a more important factor than the mean grain size. The effect of grain size on thermal conductivity is primarily linked to the number of physical contacts among soil particles (Beziat et al., 1992). Results from Zhang et al. (2015) showed that the thermal conductivity of sands, used in their study (i.e. Silica 12/20 (d50=1.029mm), Ottawa 20/30 (d50=0.783mm) and ASTM graded (d50=0.362)) may be improved with fines content and reach its maximum value at the critical fines content (F_{cr}). Critical fine content for each mixture corresponds to maximum thermal conductivity reached. In coarse sands, an increase of 30% in thermal conductivity was observed with increasing fine sands content, until the critical fines content (F_{cr}) was reached at 70% (Zhang et al., 2015).

Homogeneous distribution of bacterial cells in fine-grained soils or soils with fine content could be harder to achieve because of reduced pore space and increased filtration effect (Rebata-Landa & Santamarina, 2006; Zamani, 2017). Previous studies have indicated that filtration of bacteria through silty soils could result in a nonuniform distribution of bacteria through the soil sample with a higher concentration close to the injection port (Zamani & Montoya, 2018). The $CaCO_3$ precipitation pattern is primarily linked to the delivery and efficiency of urease activity of the injected bacteria (Barkouki et al., 2011; Van Paassen, 2009). Bacterial cells can act as nucleation sites of mineral formation during MICP ((Kirkland et al., 2021; Stocks-Fischer et al., 1999). In the soil body, bacterial cells tend to adhere to particle-particle contacts due to reduced shear stresses and a greater availability of nutrients, causing significant amount of calcium carbonate to precipitate at these locations (DeJong et al., 2010). As the bacterial cells travel through the pore space of the soil matrix, they are filtered through the soil particles with generally a log-linear reduction of microbe concentration along the injection path (Feng & Montoya, 2016; Ginn et al., 2002). The filtration effect is more prominent in case of fine-grain sands and silty sands. It was reported by Zamani (2017) that cementation distribution in 15% silty Nevada sand is less uniform compared to clean Nevada sand (d50=0.15mm). Injection of bio-cementation fluids is considered as an ideal technique for MICP treatment as it leaves room for treatment adjustments, and the injection conditions (i.e., flow, pressure, and hydraulic gradient) can be controlled during testing. On the other hand, injection method can result in uneven cementation in the soil due to inhomogeneous bacteria transport. It has been shown that, a stopped flow treatment scheme leads to a more homogeneous cementation than continuous flow injection (Martinez et al., 2013). Harkes et al. (2010) proposed that a slower injection rate of bacterial solution can allow bacteria to transport to further into the soil specimen. Whiffin et al. (2007) suggested that the increased flow rate of cementation solution allows more reagents to reach deeper locations into the treated soil column.

The change in permeability due to cementation becomes a significant issue for fine- grain sands and silty sands as it can lead to an increase in excess pore water pressure. Therefore, the allowable injection rates should be assessed considering reasonable calcium carbonate precipitation at target locations and minimizing the reduction in the permeability. Different injection strategies have been proposed to enhance the cementation uniformity of a soil sample (Cunningham et al., 2007; Gomez et al., 2017; Gunyol et al., 2022; Phillips, 2013).

Objectives

The aim of this study was to examine the effect of MICP (microbially induced calcite precipitation) techniques, using the ureolytic bacterium *Sporosarcina pasteurii* as a source of urease enzyme, on the thermal properties of silty sand. The results of the experiments and analyses provide insights into the thermal behavior of bio-cemented silty sands.

Organization

Four chapters are included in this thesis. Chapter 2 consists of a paper that was published in conference proceedings. Chapter 3 will be published later. The final chapter summarizes the main research findings and discusses future work. The remainder of this chapter describes the three chapters that compose the body of the research presented in this thesis.

Chapter 2 describes the study conducted to examine the effect of MICP, using the ureolytic bacterium *Sporosarcina pasteurii* as a source of urease enzyme, on the thermal properties of Ottawa F-65 sand. Treatment homogeneity (i.e., uniform distribution of $CaCO_3$ through the treated soil matrix) was assessed in this study. The uniformity of bio-cementation in the soil specimens were tested, and efficiency of the different injection methods and rates were investigated. Following assessment of an injection method to develop consistent mineral distribution in the specimen, thermal experiments were conducted to evaluate the alteration by MICP in the soil matrix over time and its effect on thermal properties of the sand. Details of the injection strategies developed in this and testing procedures are provided. The full reference for the paper is: Gunyol, P., M. Khosravi, A. Phillips, and K. Plymesser. 2022. 'Thermal Properties of Bio-Cemented Sand.' in, *Geo-Congress 2022*.

Chapter 3 reviews the results of a series of column experiments complemented by thermal tests to investigate the effect of MICP techniques on the thermal properties of silty sands, using the ureolytic bacterium *Sporosarcina pasteurii* as a source of urease enzyme. This chapter is to be submitted to ASCE Journal of Geotechnical and Geoenvironmental Engineering.

Chapter 4 is the conclusion and outlook section where the conclusions from evaluating the experimental data from biochemical and thermal testing assessing the potential of bio-cementation to improve geothermal properties of soil are summarized. The recommendations for the future research are presented in this section.

CHAPTER TWO

THERMAL PROPERTIES OF BIO-CEMENTED SAND

Abstract

A series of thermal experiments was conducted to investigate the effect of ureolysis-driven calcite precipitation technique using the ureolytic bacterium *Sporosarcina pasteurii* on thermal properties of bio-cemented sand. The sand used in this study was Ottawa F-65 sand and thermal properties of the sand were measured using a TR-3 sensor connected to a portable, battery-operated thermal properties analyzer. The effects of different injection methods of the injected fluids on the efficiency of calcium carbonate precipitation and the uniformity of bio-cementation through the soil specimen were investigated. The amount of urea hydrolyzed, and the amount of calcium precipitated were determined using the modified colorimetric urea assay and calcium assay, respectively. Calcium concentration along the bio-cemented soil column was determined using acid washing method followed by use of a colorimetric calcium assay. Thermal conductivity measurements were used to evaluate the changes as mineral develops in time.

Introduction

Soil thermal conductivity is the thermal conductivity of a multicomponent matrix, composed of all soil phases: air, water and solid; at various volume fractions. The use of microbially induced calcite precipitation (MICP) processes can enhance the geothermal properties of soil by altering the structural factors of soil such as mineral composition, porosity, and dry density (Whiffin et al., 2007). Urea hydrolysis, or ureolysis, is a chemical reaction which generates favorable conditions that result in the precipitation of calcium carbonate. Certain microbes or plant sources produce the enzyme urease which catalyzes the hydrolysis of urea to form carbonate ($CaCO_3$) to bond soil particles (Martinez et al., 2013; Montoya, 2012; Van Paassen, 2009; Whiffin, 2004). Cementation sites between grain particles act as highly conductive heat transfer paths by increasing the contact area between sand particles. Precipitation of calcite results in an increase in the solids content and therefore, the average dry density of the soil, by binding particles together at their contacts with calcite bridges (Whiffin et al., 2007). Calcite crystals formed around soil particles also decreases porosity. As the soil porosity decreases, the number of particle contacts could increase. Therefore, the heat path through solid particles is enhanced which results in a higher thermal conductivity of the treated soil. Recent studies have shown that precipitation of calcium carbonate through MICP process can increase the thermal conductivity of sands by up to 300% (Martinez et al., 2019; Venuleo et al., 2016). The outcome of this research is essential for the application of bio-cementation in cold environments (e.g., frost action mitigation) as it affects the thermal properties of the soil, and therefore, heat and water flow in the soil. MICP treatment of surrounding soil may also improve the efficiency of geothermal boreholes and other energy geo-structures.

The aim of this study was to examine the effect of MICP techniques, using the ureolytic bacterium *Sporosarcina pasteurii* as a source of urease enzyme, on the thermal properties of Ottawa F-65 sand. Treatment homogeneity (i.e., uniform distribution of $CaCO_3$ through the treated soil matrix) was also a critical component of this study. The uniformity of bio-cementation through the soil specimens were tested, and efficiency of the different injection methods were investigated. Following assessment of an injection method to develop consistent mineral distribution in the specimen, thermal experiments were conducted to evaluate the alteration in the soil matrix as mineral forms in time and its effect on thermal properties of the sand.

Column Design, MICP Treatment, and Testing Methods

Column Design and Set-up Figure 2.1 displays a schematic and a photograph of the PolyVinyl Chloride (PVC) column, and the thermal probe used in these experiments. Thermal properties of the soil were measured using a portable, battery-operated TEMPOS Thermal Properties Analyzer and a TR-3 sensor. The TR-3 sensor has a 100-mm long, 2.4-mm diameter needle that was inserted into the untreated specimen through the cap and kept inside the column throughout the experiment (Figure 2.1). Based on the system's manual, a minimum of 10 mm of soil material parallel to the sensor in all directions is required to avoid errors in measuring thermal properties of the soil. Thus, the MICP-treated sand specimens were prepared in columns with an inner diameter of 50-mm and a height of 120 mm, and the design allowed for evaluation of thermal conductivity over time as mineralization takes place in the sand matrix, without causing disturbance in the sand.

The inside surface of the PVC column was covered with low-friction Teflon tape to minimize the attachment of the sand to the column. Two non-corrosive wire mesh filters were placed at the bottom and top of the sand specimen to prevent intrusion of the sand material into the injection or effluent tubing. The columns were designed such that pulsed injections with resting batch reaction periods between injections of enzymes and calcium containing solutions were repeatable (i.e., flow rate and hydraulic residence time) between different specimen types. The column design also allowed for assessment of the reaction progression (for example, collection of effluent samples of the fluids to assess the urea hydrolysis and subsequent calcium precipitation). A syringe pump (KD Scientific) was used to inject solutions into the column(s).

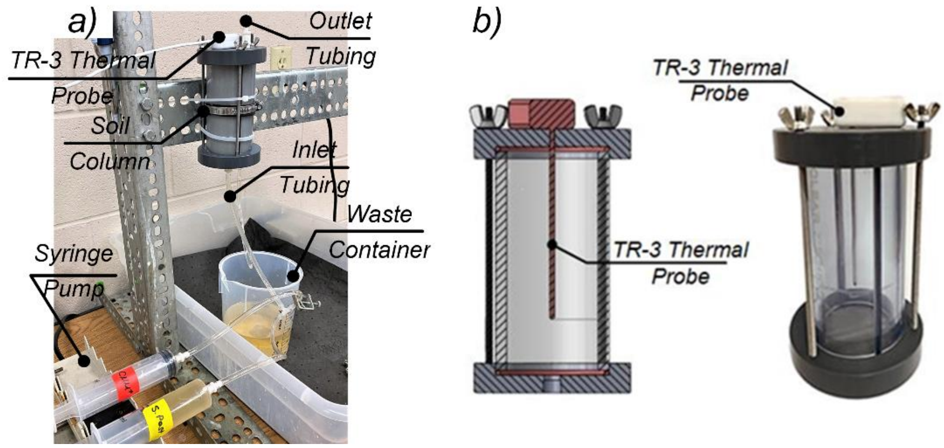

Figure 2.1. a) System setup including syringe pump, soil column, and waste container, b) a schematic, and a photograph of the column with the Thermal Probe inserted in the column

Sand Properties and Preparation The material tested was Ottawa (F-65) Sand (US Silica, Ottawa, Illinois) classified as SP (USCS ASTM 2487). Properties of the uniform sand included the following: maximum void ratio, e_{max} = 0.83; minimum void ratio, e_{min} = 0.51; specific gravity of solids, G_s = 2.65; median particle size, d_{50} = 0.20 mm. The sand specimens were compacted in cylindrical columns. Compaction were performed in eight layers with moist sand distributed evenly throughout the column for each layer. To prevent excessive compaction of lower layers, Ladd's (1978) compaction method was used (Ladd,1978). The amount of sand required for each layer was determined based on the target relative density of 50%.

Microbe Suspensions MICP promoting cultures were grown by aliquoting 1 mL of *Sporosarcina pasteurii* (ATCC 11859) from thawed frozen stock to 100 mL of filter sterilized brain-heart infusion broth (BHI, Becton Dickinson) amended with 2% urea (20 g/L urea, Fisher Scientific). The cultures were incubated overnight at 30°C on a 150-rpm shaker. After incubation, 1 mL of this culture was added to 100 mL of growth promoting media and placed on a shaking incubator at 30°C and 150-rpm, for 24 hours for use (injection into the column) the next day.

Bio-cement Promoting Solutions Bio-cementation treatments consisted of biological and cementation (CMM+) solutions. The content of each biological and cementation solution is presented in Table 2.1. Cementation solutions containing calcium were prepared with a pH value of 6.0-6.3. The biological solutions were injected into the columns following the cementation solution at intervals specified in the MICP treatment and sampling methods section.

Table 2.1. Chemical Recipe for Cementation Media

Recipe Component	Biological Solution	Cementation Solution (CMM+)
Difco Nutrient Broth	3 g/L	3 g/L
Urea	20 g/L	20 g/L
Ammonium Chloride	10g/L	10g/L
$CaCl_2*2H_2O$	-	48 g/L
S.pastuerii	+	-

MICP Treatment and Sampling Methods

After the sand specimen was compacted in the PVC column, it was disinfected by injecting 1.5 pore volumes of 70% ethanol and 10% bleach. The sand specimen was then rinsed and saturated by injecting two pore volumes of deionized water pumped into the column from the bottom port using a syringe pump prior to MICP treatment phase.

Cementation and biological fluids are injected separately in a pulsed fashion (with resting batch periods between fluid injections) to promote either precipitation or microbial growth (Phillips, 2013; Tobler et al., 2012) as needed. The pulsed injection strategy included two main phases: 1) introduction of *Sporosarcina pasteurii*, through the column, and 2) injection of a cementation solution containing urea and calcium followed by resting batch reaction periods when the flow was stopped (Whiffin et al., 2007). Through the first phase, a volume of 1.5 times the sand pore volume of the biological treatment solution, *S. pasteurii* cells grown overnight, were injected into the column to inoculate the soil with bacteria, followed by 16 hours of no-flow. In the second phase, cementation solution was injected (again a total solution volume of 1.5 times the sand pore volume) at regular two-hour intervals. Every 24 hours, a total of four injections were made, one microbial solution injection and three cementation solution injections. Four samples were collected each day for the colorimetric modified urea assay and calcium assay (Jung et al., 1975) to determine the urea and calcium concentration in samples of the fluids extracted after each batch period. Table 2.2 provides details of the MICP treatments and testing purposes for the specimens.

Table 2.2. Summary of treatments and testing purposes for MICP specimens

Specimen	***Injection Method***	***Injection Rate (ml/min)***	***Number of Pulses***	***Testing Purpose***
F0-U	Bottom Only	4	14	$CaCO_3$ Precipitation and Uniformity
F0-A-U	Alternating	4	14	
F0-A-T1	Alternating	4	16	Thermal Conductivity*
F0-A-T2	Alternating	4	32	

*$CaCO_3$ precipitation was assessed but results are not presented in detail in this study.

Two different injection methods were adopted to test the effect of injection method on the treatment efficiency of sand specimens: 1) bottom only, and 2) alternating. In the first injection method (bottom only), the biological and cementation treatment solutions were injected only from the bottom port of the specimen and injection port was not changed throughout the experiment. In the second approach, biological and cementation solutions were injected

alternatively from the top and bottom of the column by flipping the specimen. In both methods, the columns were placed vertically with upward flow direction to prevent formation of inhomogeneous cementation that might lead to occurrence of preferential flow paths along the soil matrix. The inflow rate was constant at 4 mL/min for all specimens. A summary of the soil specimens tested in this study and the injection method used for each specimen is provided in Table 2.2. Specimens treated using the alternating method are denoted with (A).
Following the MICP treatment phase, the specimens were dried in a 40 ^{o}C oven. The TR-3 sensor was kept inside the column during the drying process. The specimens were held at room temperature for two days to allow specimens to adjust back to the room temperature. After two days of waiting period, thermal conductivity values of heat treated specimens were measured.

Acid Washing and Effluent Sampling Two different approaches were used to evaluate the calcium precipitation efficiency of the two different injection methods: 1) acid washing, and 2) effluent sampling. In the first approach, acid washing, after cementation was complete and specimen was dried, the column was removed, and the remaining sand column was cut with a saw into 24 mm pieces for evaluation of the treatment homogeneity. One (1) gram of bio-cemented sand samples from each section were divided into triplicate 15 mL centrifuge tubes. Trace-metal-grade nitric acid (10%, Fisher Scientific) was added to dissolve the calcium carbonate. After the calcium carbonate was completely dissolved in acid, the liquid from the samples were analyzed via colorimetric calcium assay. In the second approach, effluent sampling, a sample of effluent was collected from the soil specimens after each batch period. The effluent samples were analyzed for calcium concentration via colorimetric calcium assay and urea concentration via a modified colorimetric urea assay (Jung et al., 1975; Phillips, 2013).

Results And Discussion

Effect of injection method on distribution of $CaCO_3$ through the specimen Uniform distribution of $CaCO_3$ along the treated soil matrix is a critical component of bio-cementation that could have a significant effect on engineering and thermal properties of the treated soil. Distribution of $CaCO_3$ precipitation may be governed by biological activity and filtration of bacteria (DeJong et al., 2010). Harkes et al. (2010) indicated that effective bacteria transport along the column has a significant impact on calcite precipitation pattern. Filtration of bacteria while the biological solution is percolating through soil particles may result in an undesired bacteria accumulation near the injection port (Harkes et al., 2010).

The calcium concentration analysis of the cemented sand sections was performed for the Specimens F0-U (Figure 2.2a) and F0-A-U (Figure 2.2b) to evaluate the cementation profile along the column length. Figure 2.2 shows the measured calcium concentration present in 1 g samples of cemented sand samples collected from five different locations along the column length. The data for the specimen F0-U exhibits gradual decrease in calcium concentration as the distance from the injection point increases. The calcium carbonate content was approximately 11 times higher at the bottom of the specimen compared to the top of the column for specimen F0-U. This significant difference in the spatial distribution is assumed to be related to filtration of bacteria through the soil (i.e., as more bacteria accumulated close to the injection port, precipitation of calcium carbonate increased at this area). The degree of filtration becomes more significant with each treatment as more suspended calcite occupies pore spaces in the soil matrix (DeJong et al., 2010).

Specimen F0-A-U displays a more homogeneous $CaCO_3$ distribution (Figure 2.2b). The filtration of bacteria is assumed to be less significant for this specimen since both top and bottom ports were used for injection of biological and cementation solutions. The loss of porosity due to bacterial flocculation and $CaCO_3$ precipitation near the inlets (top and bottom ports) may have less impact on the ability of bacteria to travel through the soil for this specimen (compared to F0-U). Therefore, more bacteria could attach to the sand grains in the core of the specimen and hydrolyze a higher amount of urea.

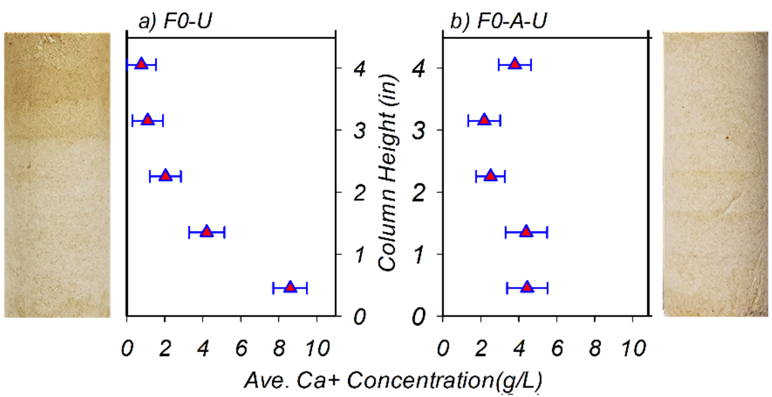

Figure 2.2. Calcium concentration analysis of the cemented of a) specimen F0-U, and b) specimen F0-A-U, showing the cementation distribution profile along the soil matrix

Figure 2.3 shows the concentration of calcium and urea from the effluent samples collected during each pulse from F0-U and F0-A-U specimens. Although both specimens received the same number of injections, there was a difference in the total concentration of urea hydrolyzed during each calcium pulse. The results from the effluent analysis showed that, for the F0-A-U specimen more than 75% of the injected calcium precipitated, while for F0-U, only 40% of the injected calcium precipitated. The difference in measured urea hydrolysis efficiency between the two specimens could be attributed to hydraulic constraints, such as bacterial flocculation, local clogging, and retarded delivery rate of chemicals due to higher cementation levels at the bottom (Al Qabany et al., 2012).

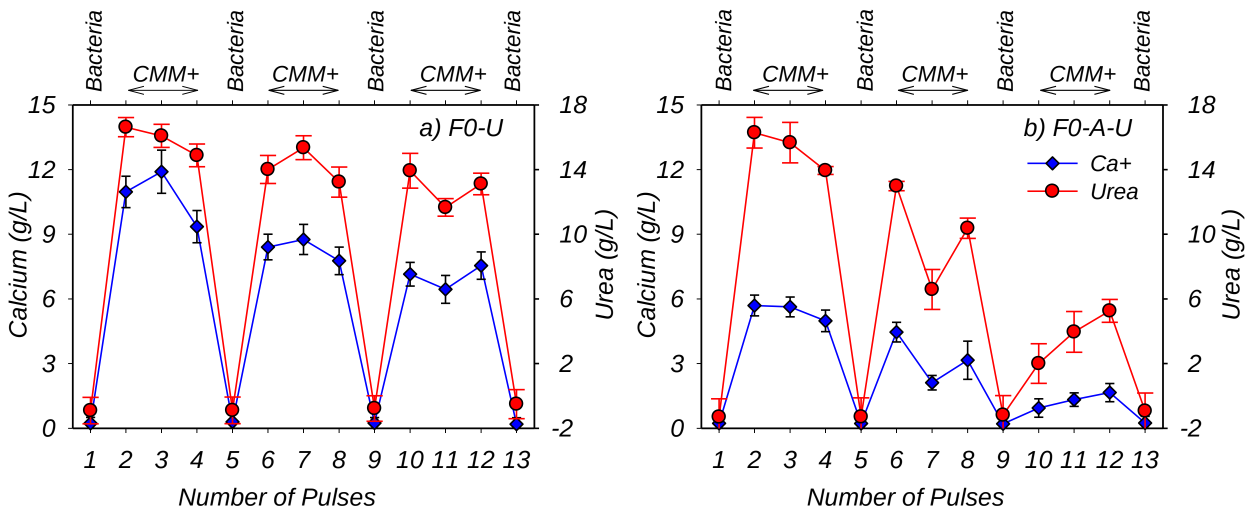

Figure 2.3. Calcium and urea concentration measurements from the effluent samples collected during each pulse (biological and cementation treatment injections) from a) specimen F0-U, and b) specimen F0-A-U, showing higher amounts of calcium and urea conversed for F0-A-U

<u>Thermal Conductivity and Thermal Resistivity Measurement</u>Thermal properties of two identical specimens, F0-A-T1 and F0-A-T2 (Table 2) are presented in Figure 2.4. The results include the thermal conductivity (k_t) throughout three different phases: 1) sand saturation phase, 2) MICP treatment phase, and 3) drying phase. During the treatment phase, the thermal conductivity of the specimens was recorded in 2-hour intervals between each cementation treatment and 16-hours after biological treatment, while for the saturation and drying stages, the thermal conductivity at the end of each were measured. The specimens remained saturated throughout the treatment stage. As summarized in Table 2, specimens F0-A-T1 and F0-A-T2 were treated with the alternating injection method and received 16 (12 cementation treatment and 4 biological treatment) and 32 pulses (24 cementation treatment and 8 biological treatment), respectively.

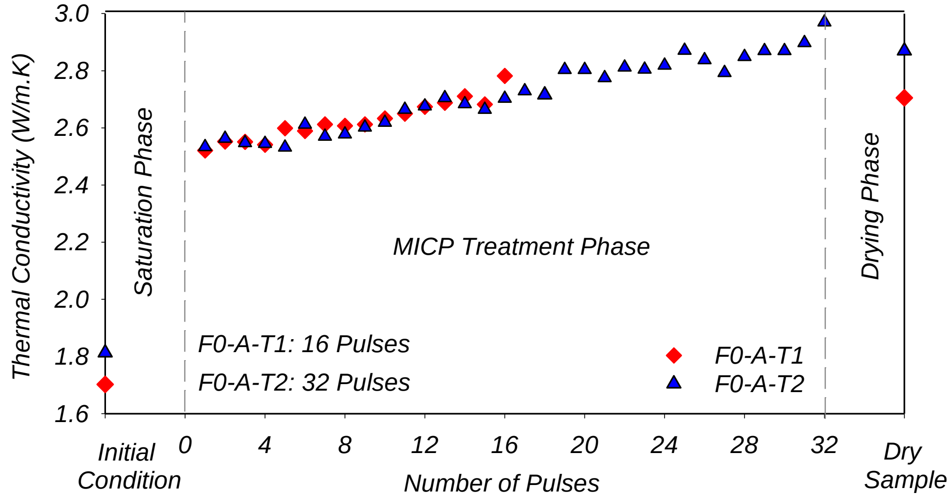

Figure 2.4. Variation of thermal conductivity (W/m.K) during the bio-cementation process of specimens with alternating injection method

As shown in Figure 2.4, the initial values of k_t for the specimens F0-A-T1 and F0-A-T2 were 1.7 and 1.8 W/m.K, respectively. After the sand specimens were saturated with deionized water prior to the bio-cementation phase, their thermal conductivity significantly increased and reached 2.52 W/m.K for specimen F0-A-T1 and 2.53 W/m.K for specimen F0-A-T2. This was expected as the thermal conductivity of the soil increases with degree of saturation as the air in voids is replaced with water. Heat transport and therefore thermal conductivity could be greatly influenced by interparticle interactions and the presence of liquids in pores. (Yun & Santamarina, 2008).

Throughout the treatment phase, the thermal conductivity of the soil specimens tended to increase with the amount of calcium precipitated around sand particles. For specimens F0-A-T1 and F0-A-T2, the value of k_t reached a value of 2.78 W/m.K and 2.97 W/m.K at the end of treatment. The increase in thermal conductivity was calculated as:

$$\Delta k_t = \left(k_{\text{t,treated}} - k_{\text{t,untreated}}\right)/k_{\text{t,untreated}}.$$

Following the MICP treatment while specimen was in a saturated condition, 12 and 24 cementation treatments resulted in Δk_t of approximately 10% and 17%, respectively. The enhancement was attributed to the formation of calcite crystals, which increased interparticle contact and thus increased heat transfer. Figure 2.5 presents the SEM images obtained for the bio-cemented specimen. The calcite crystals connecting the sand particles can be clearly observed in Figure 2.5b. Clusters of sand particles interconnected by calcite bridges are shown in Figure 2.5a from a larger scale (magnification 199X for Figure 2.5a and 1270X for Figure 2.5b).

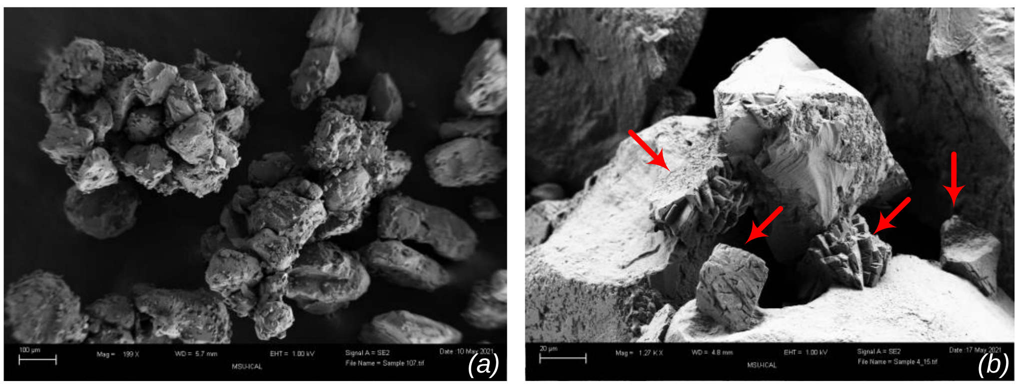

Figure 2.5. SEM images obtained for the MICP-treated specimen F0-A-U after 14 pulses of treatment: a) cluster of sand particles attached together by calcium carbonate bridges, b) calcium carbonate crystals (arrows) binding sand particles

The findings from this study have shown that bio-cementation can enhance the overall thermal conductivity (k_t) of the soil matrix by inducing the growth of calcium carbonate bridges between soil particles. The improved thermal properties of the soil treated with MICP was also attributed to the increase in the solid phase of the soil matrix. The average dry density of treated soil generally increases with the amount of precipitated calcium carbonate mass (Whiffin et al., 2007). Since calcite has greater thermal conductivity value than dry soil ($k_{t,calcite} \approx 5$ W/m.K,

$k_{t,dry-soil} \approx 0.3$ W/m.K), a decrease in soil porosity due to calcite precipitation results in an increase in thermal conduction (Martinez et al., 2019).

As expected, the measured thermal conductivity of the heat treated specimens showed a decrease in k_t by about 2.77% for specimen F0-A-T1 and 3.37% for specimen F0-A-T2 as water in the voids were replaced with air. Compared to the initial saturated condition, the porosity during the MICP treatment and the drying phases due to bio-cementation. Therefore, the drop in thermal conductivity due to drying was less than the increase in thermal conductivity due to saturation. Therefore, the effects of bio-cementation on thermal conductivity are more pronounced for dry conditions (Venuleo et al., 2016).

Conclusion

In this study, the successful development of an MICP treatment strategy to achieve efficiently uniform calcite distribution has been presented. The method was developed to evaluate the variation of thermal conductivity of bio-cemented sand using a common soil microorganism, *S. pasteurii*. Two soil columns (F0-A-T1 and F0-A-T2) were subjected to MICP treatment for thermal testing. Measurements of thermal conductivity have shown that, as the number of MICP treatment cycles increases, the amount of calcite formation increases, resulting in an enhancement in the thermal conductivity of the soil. MICP can thus offer a potential improvement technique to enhance the thermal efficiency of shallow geothermal energy as a renewable heat source. Further development of the technique for this application is needed for field implementation to improve efficacy of energy geotechnics.

CHAPTER THREE

EFFECT OF FINES CONTENT ON CALCIUM CARBONATE PRECIPITATION AND THERMAL PROPERTIES OF BIO-CEMENTED SAND

Abstract

In recent years, there has been an increasing interest in the use of biological technologies in geotechnical engineering to improve thermal properties of geomaterials. Cementation located between the grain particles acts as a highly conductive heat transfer path by increasing the contact area between the soil particles, thus resulting in an increase in thermal conductivity. Urea hydrolysis is a chemical reaction which can generate favorable conditions that result in the precipitation of calcium carbonate. Certain microbes or plant sources produce the urease enzyme which catalyzes the hydrolysis of urea to form carbonate ($CaCO_3$) to bond soil particles. In this chapter the applicability of bio-cementation via microbially induced calcite precipitation (MICP) on silty sand specimens with different fines contents of 0%, 5%, and 15% were investigated. MICP promoting fluids were injected into sand-filled columns and the resulting calcium conversion was measured. At the end of the injections, the MICP treated specimens were tested for cementation uniformity. The amount of precipitated $CaCO_3$ gradually decreased as the distance from the injection ports increased. The observed bio-cementation distribution could be attributed to the filtration of bacterial cells through the soil particles. The resulting effect of filtration on $CaCO_3$ distribution was observed to be more prominent for silty sands, presumably due to the presence of fine grains. Thermal conductivity measurements were assessed after each pulse during the MICP treatment using a TR-3 sensor. Under the saturated and untreated

conditions, thermal conductivity increased with increasing fines content. In addition, MICP treatment increased the thermal conductivity of saturated silty sands with an increasing number of treatment pulses. An increase of about 18% in thermal conductivity of the soil was achieved at an average $CaCO_3$ content of 10.7% presumably due to the formation of calcium carbonate bridges binding the soil grains together. The results presented herein suggests that MICP treatment can increase the thermal conductivity of soils in the range of fines content studied here (less than 15%). The findings of this research could be used to improve the efficiency of geothermal boreholes and other energy geo-structures by using MICP to improve the thermal conductivity of dry and partially saturated soil.

Introduction

In recent years, there has been an increasing interest in the use of biological technologies in geotechnical engineering to improve thermo-hydro-mechanical properties of geomaterials (Gomez et al., 2017; Martinez et al., 2020; Montoya & DeJong, 2015). Cementation located between the grain particles acts as a highly conductive heat transfer path by increasing the contact area between the soil particles, thus resulting in an increase in thermal conductivity. Certain microbes can alter their surrounding chemical environments to induce the precipitation of calcium carbonate, a form of bio-cement (DeJong et al., 2010; Phillips et al., 2013; Van Paassen, 2009). One mechanism that has been researched extensively is the microbe or plant produced enzyme urease, which promotes the hydrolysis of urea to change saturation conditions, which in the presence of calcium, results in the precipitation of calcium carbonate (Ebigbo et al., 2012a; Hommel et al., 2020; Mitchell et al., 2013; Phillips et al., 2016; Phillips et al., 2013). Microbially-induced calcium carbonate precipitation (MICP) in the presence of urea, the urease enzyme catalyzes the hydrolysis of urea, altering the chemical environment towards favorable conditions for precipitation of $CaCO_3$ in the presence of calcium.

$$(NH_2)_2CO + 2H_2O + Ca^{2+} \rightarrow 2NH_4^{+} + CaCO_3$$

In this process, the precipitation of $CaCO_3$, often in the stable mineral form of calcite, can bind together porous media including soil matrices. Bio-cemented sand treated by MICP has been reported to provide a reduction in soil settlement (DeJong et al., 2006; Van Paassen, 2009), an increase in soil shear strength (Chou et al., 2011a; DeJong et al., 2006; Ismail et al., 2002b), and improvement to increase soil stiffness (Feng & Montoya, 2016; Lin et al., 2016a; Montoya & DeJong, 2015b).

MICP technique has been recently proposed as an alternative for improving the thermal properties of soil (Martinez et al., 2019; Venuleo et al., 2016; Wang et al., 2020; Xiao et al., 2021). Heat transfer in soil takes place primarily through conduction, and flow of heat is largely controlled by the contacts between the solid particles. MICP technique alters the structural make-up of the soil and the nature of the interparticle contacts through calcium carbonate precipitation, and hence can increase the overall thermal conductivity of the soil matrix. Precipitation of calcite results in an increase in the solids content and therefore, the average dry density of the soil through the process of binding particles together at their contacts by calcite bridges (Whiffin et al., 2007). Calcite crystals formed around soil particles increase the number of particle contacts and enhance heat transfer paths through solid particles resulting in higher thermal conductivity of the treated soil (Venuleo et al., 2016). MICP treatment of sand could lead to an increase in soil thermal conductivity of up to 250% (Venuleo et al., 2016) particularly in dry and partially saturated soils. Under dry conditions, the calcite crystals replace the air which could significantly increase the thermal conductivity of the soil. The increase in overall thermal conductivity in percentage is more pronounced at lower degrees of saturation. The 6.7% increase in calcium carbonate led to 330% increase in thermal conductivity at the degree of saturation, S_r = 0%, the increase in thermal conductivity was 37% at S_r = 10% (Martinez et al., 2020). Previous studies on the effect of bio-cementation on soil thermal behavior have mainly focused on thermal properties of medium sand (e.g., median size of 0.2 mm). However, the thermal properties of bio-cemented soil as a function of the amount of $CaCO_3$ formed and fines content requires further investigation. Presence of fine-grained soil (e.g., silt) in the soil matrix adds complexity to applicability of MICP technique to enhance thermal properties of soil due to smaller pore sizes and larger specific surface areas (Zamani & Montoya, 2018).

The impact of grain size on thermal conductivity is primarily linked to the number of physical contacts among soil particles (Beziat et al., 1992). The increase in thermal conductivity with increasing fines content is expected to continue until the sand-silt granular mixture reaches its maximum dry density. Zhang et al. (2015) mixed sands with different median particle size, Silica 12/20 (with median particle size, d_{50}=1.03 mm), Ottawa 20/30 (with d_{50} = 0.78 mm) and ASTM graded (d_{50} = 0.36 mm), and observed that the thermal conductivity of sand increased with fines content. The results suggested that thermal conductivity of the mixed sand initially increased up to a critical fines content (F_{cr}) due to more efficient interparticle contacts and contacts per unit volume. For the coarse sand material tested (Silica 12/20 with median particle size, d_{50}=1.03 mm), the critical fines content was 70% and a 30% increase in thermal conductivity was observed.

Although presence of fines could improve thermal properties of soil, previous studies have indicated that homogeneous distribution of bacterial cells in fine-grained soils or soils with fines content could be harder to achieve due to the reduction in pore spaces and the increase in filtration effect (Rebata-Landa & Santamarina, 2006; Zamani, 2017). The $CaCO_3$ precipitation pattern is primarily linked to the delivery and efficiency of urease activity of the injected bacteria (Barkouki et al., 2011; Van Paassen, 2009). Bacterial cells can act as nucleation sites of mineral formation during MICP (Kirkland et al., 2021; Stocks-Fischer et al., 1999). Bacterial cells tend to adhere to particle-particle contacts due to reduced shear stresses and a greater availability of nutrients, causing a significant amount of calcium carbonate to precipitate at these locations (DeJong et al., 2010). As the bacterial cells are traveling through the pore space of the soil matrix, they are filtered through the soil particles with generally a log-linear reduction of microbe concentration along the injection path (Feng & Montoya, 2016; Ginn et al., 2002). Filtration of bacteria through silty soils could result in a nonuniform distribution of bacteria through the soil sample with a higher concentration close to the injection port (Zamani & Montoya, 2018). Based on Zamani (2017), cementation distribution in silty Nevada sand with 15% silt is less uniform when compared to the clean Nevada sand (d_{50} = 0.15mm).

Injection and premixing methods have been proposed to enhance the treatment uniformity of a soil with fines content (Cunningham et al., 2007; Gomez et al., 2017). The injection method allows for the flushing of bacterial solution and a retention period for bacteria to attach to the soil particles before injection of the cementation solution. In the premixing method, the bacteria are mechanically mixed with the soil before introducing the cementation solution. Injection method is considered the ideal technique for MICP treatment method as it leaves room for treatment adjustments, and the injection conditions (i.e., flow, pressure, and hydraulic gradient) can be controlled during testing (Ginn et al., 2002; Harkes et al., 2010; Martinez et al., 2013; Whiffin et al., 2007).

This paper summarizes the results of a series of column experiments analyzed to investigate the effect of MICP techniques, using the ureolytic bacterium *Sporosarcina pasteurii* as a source of urease enzyme, on the thermal properties of silty sands. The column experiments were carried out at the Center for Biofilm Engineering Lab (CBE) and the geotechnical/geothermal tests were executed at the Geotechnical Lab in the Department of Civil Engineering, both at Montana State University. Ureolytic bacterium *Sporosarcina pasteurii* was used as a source of urease enzyme. Following the assessment of treatment homogeneity (i.e., uniform distribution of $CaCO_3$ through the treated soil matrix), thermal experiments were conducted to evaluate the alteration in the soil matrix as mineral formed over time and its effect on thermal properties of the sand. The results of the experiments and analyses provide insights into the thermal behavior of bio-cemented silty sands.

Materials and Methods

All soil specimens were prepared in columns with an inner diameter of 50-mm and a height of 120 mm. Figure 3.1 displays a schematic and a photograph of the PolyVinyl Chloride (PVC) column. The thermal probe used to measure thermal conductivity of soil samples was a portable, battery-operated TEMPOS Thermal Properties Analyzer and a TR-3 sensor. The TR-3 sensor is a 100-mm long, 2.4-mm diameter needle that was inserted into the untreated specimen through the cap and kept inside the column throughout the experiment (Figure 3.1). The design allowed for evaluation of thermal conductivity over time as mineralization takes place in the sand matrix, without causing disturbance in the soil. A minimum of 10 mm of soil material parallel to the TR-3 sensor probe in all directions was required to avoid errors in measuring thermal properties of the soil. The inside surface of the PVC column was covered with low-friction Teflon tape (Low-Friction FEP Tape, McMaster-Carr) to minimize attachment of sand to the PVC. A non-corrosive wire mesh filters was placed at the bottom and top of the sand specimen to prevent intrusion of the sand material into the injection or effluent tubing.

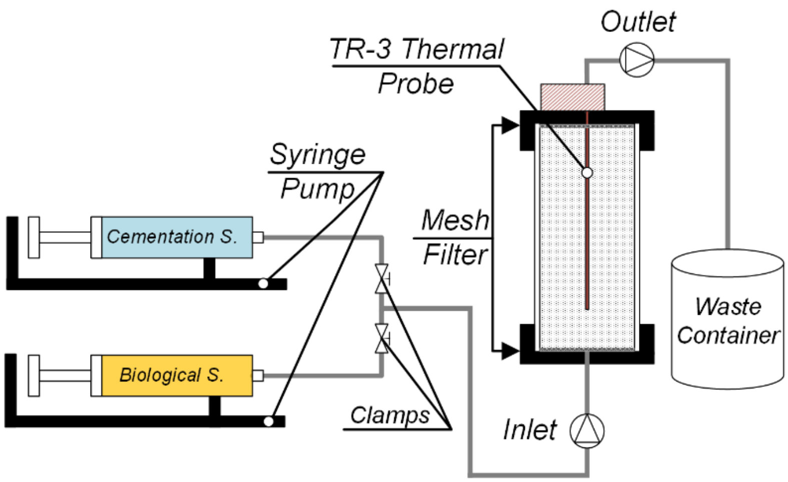

Figure 3.1. Schematic of the setup including the column with the thermal probe, treatment solutions (biological and cementation solutions) and a syringe pump (KD Scientific) to inject solutions into the column(s)

The laboratory testing program characterized soil samples of Ottawa F-65 Sand (US Silica, Ottawa, Illinois) mixed with 0%, 5%, and 15% silt (Sil-Co-Sil 250 obtained from U.S. Silica in 2020) (by weight). Ottawa sand is a uniform white silica sand classified as SP (USCS ASTM 2487) with rounded grains, a quartz content of 99.7%, and minimal fines (US Silica 2016). Properties of the uniform sand included the following: maximum void ratio, e_{max} = 0.83; minimum void ratio, e_{min} = 0.51; specific gravity of solids, G_s = 2.65; median particle size, d_{50} = 0.20 mm. Sil-Co-Sil 250 is a highly granular, non-plastic silt with a quartz content of over % 99.5. The material is low in moisture, chemically inert, and acid resistant. Properties of the silt material included the following: G_s = 2.75; plasticity index, PI=0 (Price, 2018, U.S. Silica). The amount of soil required for each layer was determined based on the desired density. Compaction of the sand in the PVC column was performed in eight lifts with moist soil (a moisture content of 7%) distributed evenly throughout the column for each layer. To prevent excessive compaction of lower layers, Ladd's (1978) compaction method was used.

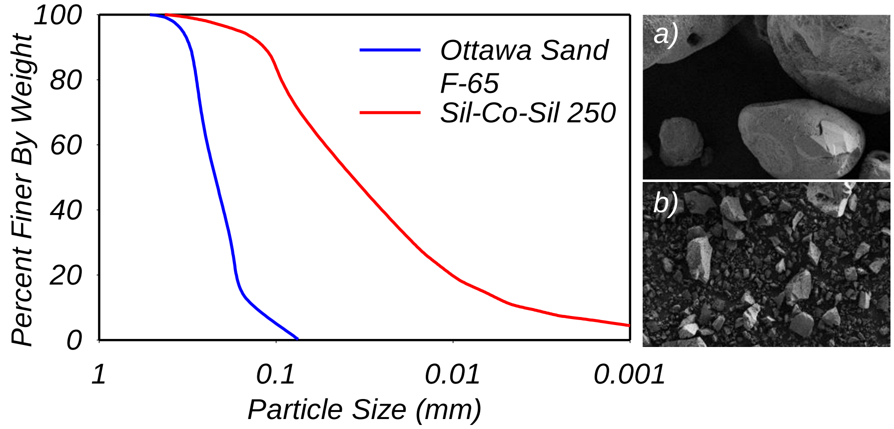

Figure 3.2. Particle size distribution and SEM images of a) Ottawa sand F-65 (20 μm) b) Sil-Co-Sil 250 (100 μm)

Thermal experiments were conducted at three stages. After the soil sample was prepared in the column, the TR-3 sensor was inserted into the untreated moist soil and the thermal conductivity of the soil was measured. The samples were then saturated with deionized water. The saturated columns were subjected to MICP treatments, and a control column was treated only with deionized water, without bacteria, urea, or calcium sources. Prior to injection of treatments, a starter culture was prepared by aliquoting 1 mL of *Sporosarcina pasteurii* (ATCC 11859) from thawed frozen stock to 100 mL of filter sterilized Brain-Heart Infusion broth (BHI, Becton Dickinson) amended with 2% urea (20 g/L urea, Fisher Scientific). The cultures were incubated overnight at 30°C on a 150-rpm shaker. Following incubation, 1 mL of this culture was added to 100 mL of growth promoting media for 24 hours for injection into the column the next day (bacterial solution). Following the first injection, a certain volume of a cementation solution (CMM+) containing 3 g/L nutrient broth, 20 g/L urea, 10 g/L ammonium chloride, and 48g/L $CaCl_2*2H_2O$ was applied to the specimens.

MICP Treatment

Injection Strategy

The columns were designed such that pulsed injections with resting batch reaction periods between injections of enzymes and calcium containing solutions were repeatable (i.e., flow rate and hydraulic residence time) between different specimen types. The pore volumes of the specimens were measured by injecting DI water into the specimens, and subtracting the tubing volume from the total volume of water used. The compacted specimens were disinfected prior to the experiment by injecting 1.5 pore volumes of 70% ethanol and 10% bleach. The specimens were then rinsed and saturated by injecting two pore volumes of deionized water prior to MICP treatment phase. Biological and cementation solutions (1.5 pore volumes) were injected alternatively from the top and bottom of the column by flipping the specimen in order to achieve uniform distribution of cementation. The volume of injection fluids per pulse were 100 mL for 0% fines specimen, 95 mL for 5% fines specimen, and 85 mL for 15% fines specimen. The injection rate was held constant at 4 mL/min throughout the experiments for comparison purposes. The system was not monitored for pressure increase. A summary of the soil specimens tested in this study and fines content for each specimen is presented in Table 3.1.

Table 3.1. Detailed injection program used in the MICP specimens

Specimen	*Fines content (%)*	*Number of Pulses*	*Injection Volume(mL)**
F00-P16	0.0	16	100
F00-P32	0.0	32	100
F05-P32	5.0	32	95
F15-P16	15.0	16	85
F15-P32	15.0	32	85

*The volume of injected treatment solutions decreased with increasing fines content as the amount of treatment solutions were determined based on the actual pore volume of the specimens (1.5 times of the actual pore volume). The specimens initially had approximate measured pore volume of 66 mL for F00, 63 mL for F05, and 55 mL for F15.Table 3.2 provides the details of the injection program for the treatment solutions. Specimens denoted with 32P were subjected to 24 pulses of CMM+ and 8 pulses of biological treatments. Specimens denoted with 16P received only 12 pulses of CMM+ and 4 pulses of biological treatments. Following the MICP treatments, the specimens were dried in a 40 ºC oven for further analysis.

Table 3.2. Detailed injection program used in the MICP specimens

Number of Days	**Treatment Solution**	**Duration (hr)**	**Flow Rate*(mL/min)***
1	Bacterial Solution	18	4
2+	CMM+ CMM+ CMM+ Bacterial Solution	2 2 2 18	4 4 4 4
Termination Day	CMM+ CMM+ CMM+	2 2 2	4 4 4

<u>Ca^{2+} concentration determination: Effluent fluid sampling</u> The column design allowed for assessment of the reaction progression (for example, collection of effluent samples of the fluids to assess the urea hydrolysis and subsequent calcium precipitation). A sample of effluent was

collected from the fluids that were in the soil specimens after each batch period. The effluent samples were analyzed for calcium concentration via colorimetric calcium assay and urea concentration via a modified colorimetric Jung assay (Freiling Z., 2019, Jung et al., 1975; Phillips, 2013).

$CaCO_3$ determination: Acid washing cemented specimen $CaCO_3$ content was determined using a gravimetric acid washing method. Following the thermal conductivity testing, the specimens were divided into 5 sections along the length of the flow path. Each section was crushed to powder using a grinder. Then 1 g sample was added to 5 mL of 10% (V/V) HNO_3 to allow for $CaCO_3$ to be dissolved. The mass of $CaCO_3$ was calculated by measuring the difference between oven-dried mass of the soil sample before and after the acid washing process.

Microstructure Analysis Samples from MICP-treated columns with 0%, 5% and 15% fines content, and the control were saved for further analysis through microscopy imaging. Zeiss SUPRA 55VP field emission scanning electron microscopy (FE-SEM) and energy dispersive spectroscopy (EDS) were conducted using JEOL JSM-6100 system (ICAL, Bozeman, Montana). Voltage used was 1.00 KV for imaging. The Energy-Dispersive x-ray Spectrometer (EDS) was used to generate characteristic x-rays to examine individual elements encountered.

Results and Discussion

The results of a series of column experiments are presented to illustrate the effects of fines content on the distribution of bio-cementation and thermal properties of bio-cemented sandy silt. The results include calcium carbonate precipitation profiles and the evaluation of thermal conductivity of MICP treated sand specimens (Ottawa F-65) with 0%, 5%, and 15% fines content (Sil-Co-Sil 250) content.

<u>Effect of fines content on calcium carbonate distribution and precipitation</u>

Figure 3.3 shows the cumulative Ca^{2+} (g) conversion calculated based on the concentration of calcium data from the effluent samples collected during each pulse compared to the concentration in the injected fluids (influent). The total Ca^{2+} injected in the specimens were 31.4 g for F00, 28.8 g for F05 and 26.7 g for F15 specimens. The results show that the calculated Ca^{2+} conversion was the highest for the specimen with 0% fines (~ 22.6 g) and lowest for the specimen with 15% fines (~ 16.3 g).

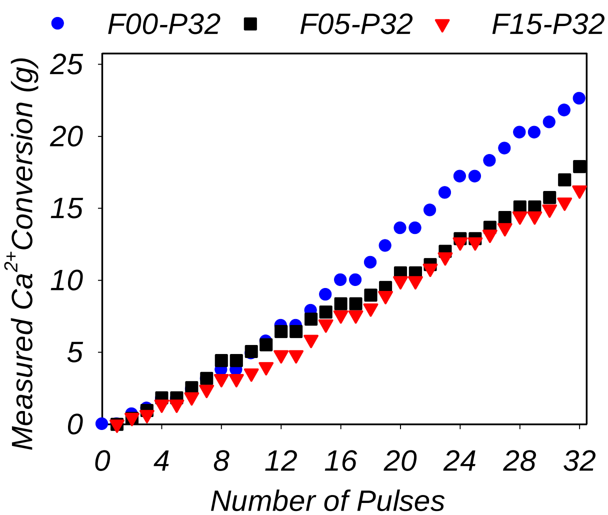

Figure 3.3. Ca^{+2} (g) conversion measured from effluent sampling for specimens with 0%, 5% and 15% fines content

The results from the acid digestion method indicate that the amount of total $CaCO_3$% present within the specimen was the lowest in the specimen with 15% fines and the highest in for the specimen with 0% which agrees with the predicted from effluent sampling. The specimen with 15%, 10%, and 0% fines had an average $CaCO_3$ of 10.7%, 9.23%, and 7.16%, respectively.

The results from the effluent sampling and post-treatment acid digest methods confirm each other. Lower precipitation in sample with fines content were expected as the samples with higher silt content had lower measured pore volume, and thus received a smaller amount of injection fluids.

The $CaCO_3$ content distributions of specimens with 0%, 5% and 15% silt content for specimens receiving 32 and 16 pulses are presented (Figure 3.4 A, B). For all specimens the amount of precipitated $CaCO_3$ gradually decreases as the distance from the top and bottom injection ports increases. For the specimens that received 32 pulses, the average amount of $CaCO_3$ present in 1 gr samples ranged between (14.67-11.57)% for the section near the bottom port, (8.32-3.26)% for the mid-section, and (10.73-8.69)% for the top injection port.

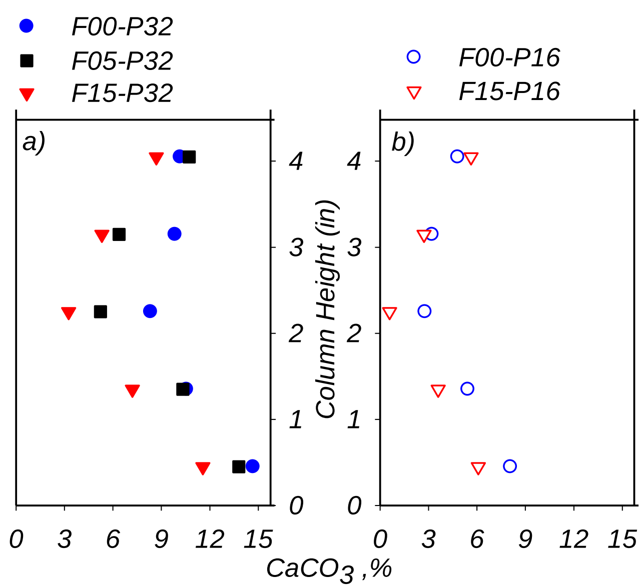

Figure 3.4. Calcium carbonate profile along the column length for specimens with 0%, 5% and 15% fines content receiving 32 pulses (a) and 16 pulses (b)

The observed bio-cementation distribution along the soil height could be attributed to the filtration of bacterial cells through the soil particles, resulting in a higher amount of $CaCO_3$

precipitation at the top and the bottom layers (Whiffin et al., 2007). $CaCO_3$% differences of bottom to middle sections were 6.35 % and 8.31% for F00-P32 and F15-P32 specimens. Therefore, the reduction in cementation towards the middle of the specimen, becomes more pronounced as the fines content increases. The trend is as expected since the filtration criteria of soil structure becomes more prominent with increased fines in the soil matrix. Due to the reduced volume of pore space that is occupied by the fine particles, filtration of bacterial cells could increase. Permeability reduces with increasing fines content (Zamani & Montoya, 2018) and due to $CaCO_3$ precipitation as the number of treatments increase. Cheng et al. (2013) reported 5.2 $m/s \times 10^{-5}$ reduction in hydraulic conductivity with 15% $CaCO_3$ content. Reduced permeability obstructs the flow and results in slow transport of injected fluids, allowing more time for urease activity around the injection points. Additionally, flow velocity is directly related to the adsorption and filtration of bacteria (Foppen & Schijven, 2006). Slower flow velocities could allow for more bacteria to attach on the particle surfaces (Gunyol et al., 2022; Harkes et al., 2010). Potentially, a larger concentration of bacteria around the injection ports can hydrolyze a higher amount of urea, resulting in a localized precipitation of $CaCO_3$ in all specimens with more pronounced effect with the specimens with fines content.

The uniformity in cementation distributions improved by increasing the number of the pulses from 16 to 32. The improvement in uniformity was more pronounced for the specimen with 15% fines content. By increasing the number of treatments from 16 to 32 pulses, the $CaCO_3$% (g/g) at the mid height of the specimen F15, increased 5.5 times in F15-P32 specimen compared to F15-P16 whereas this increase was only 2.9 times in the specimen F00-P32 compared to F00-P16. Higher increase of $CaCO_3$% in the middle section of the specimen with

15% fines might be due to the movement of loose calcium carbonate crystals and cemented silt particles as suggested by Zamani and Montoya (2018) the precipitated $CaCO_3$ around the silt particles might form silt aggregates that can easily detach from the sand grains. Additionally, using the same injection rate for all samples might have forced injected fluids to travel faster through the smaller pore voids and cause intergranular fractures in already cemented soil particle clusters. For both F00 and F15 specimens, the fractured $CaCO_3$ bridges, may allow for more bacteria to reach further points from the injection point and attach to the grain particles in the middle section of the specimen. This disruption can result in a better distribution of urease activity over the column length resulting in a more uniform condition.

Effect of calcium carbonate precipitation and fines content on thermal properties

Figure 3.5 shows the variation of thermal conductivity measured at the initial condition and after each pulse. The results include the thermal conductivity (k_t) throughout three different phases: 1) soil saturation phase, 2) MICP treatment phase, and 3) one week oven drying phase . During the treatment phase, the thermal conductivity of the specimens was recorded in 2-hour intervals between each cementation treatment and 16-hours after biological treatment, while for the saturation stage, the thermal conductivity at the end of each were measured. The specimens remained saturated throughout the treatment stage. The specimens had an initial water content of 7% for compaction. Three untreated control soil specimens with 0%, 5% and 15% fines were placed in an oven after compaction and their thermal conductivities were measured. The dried untreated control soil specimens (0% water content) with 0%, 5% and 15% fines had thermal conductivity values of 0.22, 0.24 and 0.26 W/m.K, respectively. Figure 3.5 also includes the thermal conductivity of an untreated soil saturated with deionized water with k_t = 2.48 W/m.K as a control sample. Thermal conductivity of deionized water was similar to the thermal properties of other pore filling fluids (cementation solution with k_t = 2.44 W/m.K and biological solution without *S. pasteurii* with k_t = 2.52 W/m.K). Therefore, the control specimen was run with DI water only.

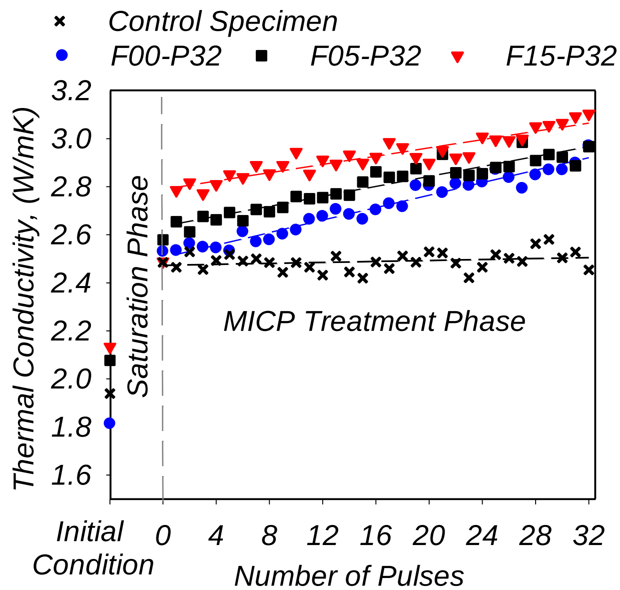

Figure 3.5. Variation of thermal conductivity (W/m.K) during the saturation and MICP treatment phases of specimens with 0% (F00), 5% (F05) and 15% (F15) fines content that received 32 treatment pulses, and the control specimen

As shown in Table 3.4., the initial values of k_t for the untreated specimens with 7% water content and 0%, 5% and 15% fines were 1.81, 2.08, and 2.13 W/m.K, respectively. The results showed a rapid increase in thermal conductivity when the samples were saturated and the air (k_{air}~0.02 W/m.K) in the pore space in the soil matrix was replaced with water (k_{water}~0.3 W/m.K). Table 3.3 provides a summary of the thermal conductivity measurements of the samples with varying fines content.

Table 3.3. Summary of thermal conductivity measurements (W/m.K)

	0%	**7% Initial**	**Saturated Untreated**	**Saturated Treated**
F0	0.22	1.81	2.53	2.97
F5	0.24	2.08	2.65	2.97
F15	0.26	2.13	2.78	3.10

Under the saturated and untreated conditions, thermal conductivity increased with increasing fines content. The observed increase with the addition of fines when compared to the specimen with 0% fines at the untreated condition, is approximately 5% for the specimen with 5% fines, and 10 % for the specimen with 15% fines. This is attributed to the presence of silt located between sand particle contact points which can result in a higher number of heat transfer paths through increased contact points.

As shown, thermal conductivity increases with the number of pulses for all specimens when compared to the control saturated specimen treated with DI water. For the untreated saturated sample, the difference between the thermal conductivity of samples F00-P32 and F15-P32 is 0.25 W/m.K and for the bio-treated sample, the difference between the two is only 0.14 W/m.K. Therefore, results indicate that the effect of fines content on thermal conductivity is reduced by increasing the number of pulses. The observed behavior could be attributed to the increase in the solid mass in the soil matrix due to $CaCO_3$ precipitation. Since the volume of treatments that were received by the specimens were calculated based on the initial pore volume in the specimens, a larger amount of $CaCO_3$ precipitation was needed to fill the pore spaces between the grain particles for the F00, F05 and F15 specimens, respectively, as the initial pore volume decreased with increasing fines content.

Figure 3.6 shows the evaluation of thermal conductivity with calculated cumulative Ca^{2+} (g) conversion. The Ca^{2+} conversion was calculated based on the difference between the Ca^{2+} injected (CMM+, cementation solution) and the Ca^{2+} concentration measured in the effluent samples. Increasing Ca^{2+} conversion possibly indicated a higher amount of $CaCO_3$ precipitation (i.e., increase in solid mass in the soil matrix). The increase in thermal conductivity under saturated conditions are calculated as $\Delta k_n = (k_{treated\_n} - k_{untreated})$, where n is the number of pulses, $k_{untreated}$ is the thermal conductivity of the saturated untreated specimen, and $k_{treated\_n}$ is the thermal conductivity of saturated treated specimen after n pulses.

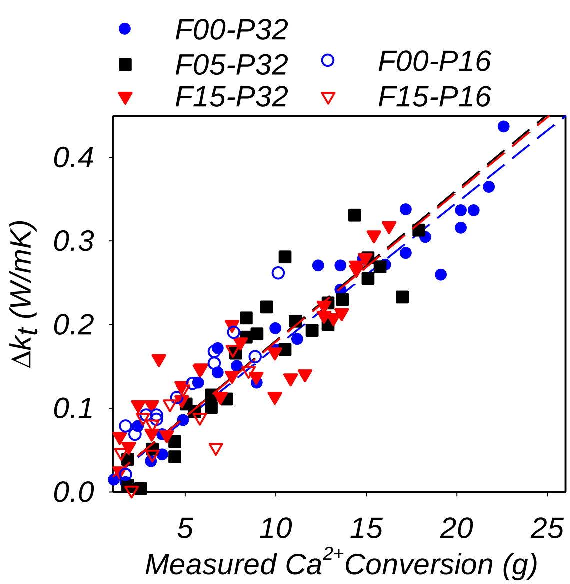

Figure 3.6. Variation of thermal conductivity versus Ca^{+2} (g) conversion for all specimens with varying fines content that received 32 and 16 treatment pulses, showing similar rates of increase in thermal conductivity

A clear positive correlation is observed between the calcium conversion and the increase in thermal conductivity for all specimens with varying fines content. The reduction in porosity in the soil matrix due to $CaCO_3$ precipitation plays the governing role in the increase in thermal conductivity (Yun & Santamarina, 2008). $CaCO_3$ crystals binding the grains, increases the crosssectional area of the contact points between the particles, resulting in reduction of the intergranular thermal resistivity. Through SEM imaging the grains were observed to be bonded together by $CaCO_3$ bridges acting as conductive paths ($k_{calcite}$ ~5 W/m.K) where heat can transmit in the inter-grain region (Figure 3.7).

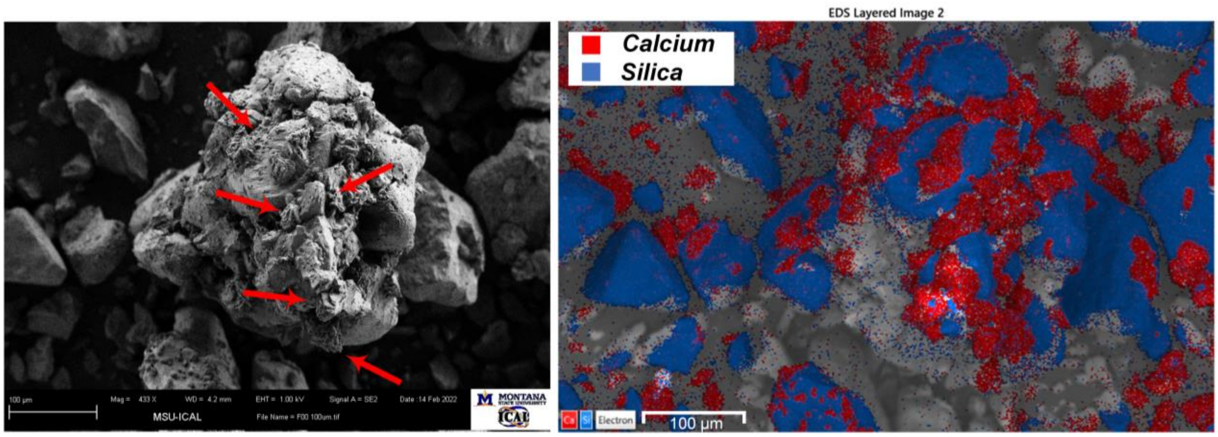

Figure 3.7. SEM image of the sand cluster taken from MICP treated specimen with 0% fine content (100 µm) on the left and EDS image of the same specimen on the right. On the SEM image the red arrows are showing the $CaCO_3$ bridges connecting the sand particles together, forming a sand cluster. On the EDS image, calcium and silica are indicated by false red coloring and false blue coloring, respectively

Figure 3.8. presents the change in the thermal conductivity versus average $CaCO_3$% present in the specimens. The average $CaCO_3$% presented in this figure was calculated based on the amount of $CaCO_3$% present in the soil along the thermal probe length. Results showed that the change in thermal conductivity Δk defined as $k_{treated} - k_{untreated}$ follows an increasing trend as the $CaCO_3$ precipitation in the soil matrix increases. $k_{treated}$ and $k_{untreated}$ are thermal conductivities of saturated treated and saturated untreated specimens. The maximum Δk after bio-cementation was 0.44 W/m.K (17% increase in thermal properties) in this study, for the specimen F00-P32at 9.7% $CaCO_3$. The increase in thermal conductivity values were determined as 0.436 W/m.K for F00-P32, 0.313 W/m.K for F05-P32, 0.318 W/m.K for F15-P32.

For comparison purposes, a summary of testing method details of previous studies on thermal conductivity of bio-cemented soil are presented in Table 3.4. When findings in this study are compared to the literature (Figure 3.8), the results show variance as to the increase in thermal conductivity versus $CaCO_3$% content present in the samples. The equations *(A-B)/A x 100 and *(A-B)/A x 100 are two different the formulas used to calculate the $CaCO_3$ percentage in the specimens tested in the studies presented. The mass of original oven-dried sand sample is denoted with (A) and the mass of post acid washing sand sample (B) without calcium carbonate is denoted with (B). However, the results from this study was consistent with Martinez et al. (2019). The increase in thermal conductivity (*Δk)* reported by Martinez et al. (2019) was 0.44 W/m.K at 6.72% $CaCO_3$ using Ottawa 50-70 sand with a mean particle size of 0.26 mm. The same amount of increase, *Δk* of 0.44 W/m.K was reached at 9.7% $CaCO_3$ using Ottawa F-65 sand with a mean particle size of 0.2 mm.

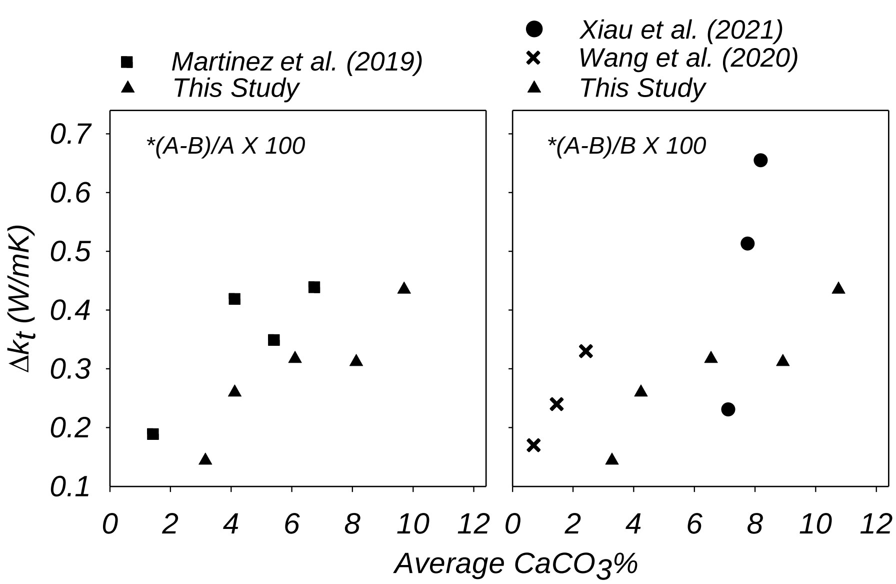

Figure 3.8. Change in thermal conductivity with average calcium carbonate content along the probe length (Original oven-dried sample (A) and post acid washing sand sample without calcium carbonate (B)). On the left, the data presented are from the studies that used the

equation*(A-B)/A×100 for $CaCO_3$ content calculation, on the right the data presented is from the studies that used the equation*(A-B)/B×100 for $CaCO_3$ content calculation

Table 3.4. Summary of previous studies

Author	Thermal Testing Method	Relative Density	D50	Specimen Dimensions	$CaCO_3$ Content Calculation (%)
Martinez	TR-1 needle sensors	90	0.26	D:70mm, H:140mm	*(A-B)/A×100
Xiau	Hot Disk Thermal Analyzer	35	0.77	D:65mm, H:20 mm	*(A-B)/B×100
Wang	Dual probe heat pulse (DPHP)	80	0.35	D:39mm, H:50mm	*(A-B)/B×100
This study	TR-3 Probe	50	0.2	D:50mm, H:120mm	*(A-B)/A×100

* Original oven-dried sample (A) and post acid washing sand sample without calcium carbonate (B)

It should be noted that, the direct comparability of the thermal conductivity measurements and $CaCO_3$% content depends on the thermal testing method, soil parameters, specimen size and $CaCO_3$ content measurement and calculation methods. Additionally, different injection strategies (i.e., flow rate, flow direction, urea/calcium concentration etc.) can yield different $CaCO_3$ precipitation patterns which may also result in deviation in thermal conductivity data.

Statistical Analysis

To determine the statistical significancy of the results, an ANOVA test was performed. Three main questions were evaluated using ANOVA test: 1) Does fines content have an effect on the thermal conductivity (k_t), 2) Does Ca^{2+} conversion effect thermal conductivity (Δk_t) of treated soil, and 3) Does the effect of Ca^{2+} conversion of the increase of thermal conductivity (Δk_t) depend on the fines content. The use of regression analysis involves certain key assumptions, including independence between groups and individuals, normality of residuals, linearity of residuals and homogeneity of variance. Figure 3.9 presents the diagnostic plots used to confirm ANOVA assumptions.

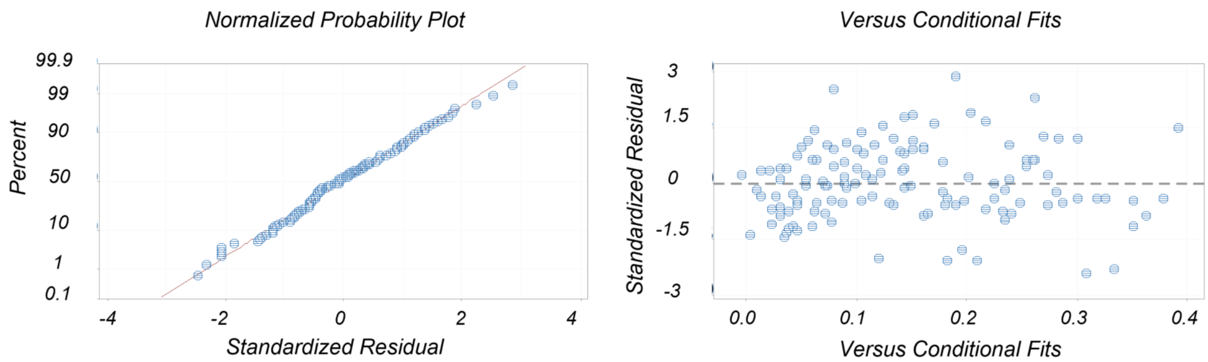

Figure 3.9. Conditional residual plot for the increase of thermal conductivity (Δk_t)

To determine whether fines content of 0%, 5% and 15% have an effect on the thermal conductivity (k_t) of untreated/treated soil three different comparison approaches were used. When the thermal conductivity values at Ca^{2+} =0 (untreated condition) were analyzed, it was observed that F15 had the highest mean thermal conductivity at Ca^{2+} =0 with a k_t value of 2.75 W/m.K, this value was 2.65 W/m.K for F05 sample and 2.55 for F00 with a p-value of 0.120, suggesting there is no statistically significant difference in the thermal conductivity values of untreated specimens with different fines content. When the k_t values of the samples were averaged over all Ca^{2+} values, F15 still resulted in the highest mean thermal conductivity value of 2.877 W/m.K, this value was 2.792 W/m.K for F05 sample and 2.678 for F00 specimen with p-values more than or equal 0.118, suggesting no statistically significant difference in the thermal conductivity values of MICP treated specimens with different fines content. The rate of increase in thermal conductivity (k_t) of the samples were determined as; 0.0159 for F15, 0.0185 for F05, and 0.01722 for F00 with a p-value of 0.259, suggesting no statistically significant difference in the rate of increase in thermal conductivity for the specimens with different fines content.

The results of the ANOVA test suggest that there is a statistically significant effect of the Ca^{2+} conversion on the increase of thermal conductivity (Δk_t) of treated soil. It was determined that the thermal conductivity increases for 17 W/m.K for every 1000g Ca^{2+} converted with a p-value less than 0.0001 and 95% confidence interval. To determine whether the effect of Ca^{2+} conversion on the increase of thermal conductivity (Δk_t) depend on the fines content, the mean Δk_t values were determined as 0.1498 W/m.K for F00, 0.1406 W/m.K for F05, and 0.1379 W/m.K for F15 with p-values more than or equal 0.814. Therefore, the analysis provided enough evidence that the effect of Ca^{2+} conversion on the increase of thermal conductivity (Δk_t) does not depend on the fines content for the range of fines content studied here.

Conclusion

A series of column experiments were to investigate the effect of fines content on bio-cementation process and thermal properties of bio-cemented silty sand. Ureolytic bacterium *Sporosarcina pasteurii* was used as a source of urease enzyme. The results were used to investigate the calcium carbonate precipitation profile and the evaluation of the thermal conductivity of MICP treated silty sand specimens (with fines contents of 0%, 5%, and 15%).

Five soil columns were subjected to MICP treatment, resulting in a similar cementation pattern within the columns for all specimens with higher concentration at the injection port and lower concentration at the middle of the specimen. Measurements from effluent sampling and post-treatment acid digest methods showed a lower precipitation with increasing fines content. The average calcium carbonate content ranged between 7.2% for F15-P16 with 15% fines content and 10.7% for F00-P32 with 0% fine. This was expected as the samples with higher silt content have lower pore volume and received lower amount of injection fluids. For all specimens, the amount of precipitated $CaCO_3$ gradually decreases as the distance from the top and bottom injection ports increases. This was attributed to the filtration of bacterial cells through the soil particles, resulting in a higher cementation near the injection points.

Measurements of thermal conductivity were obtained prior to and during MICP treatment. Thermal conductivity increased with the number of pulses for all specimens when compared to the control specimen. Under the saturated and untreated conditions, thermal conductivity increased by about 11% when fines content was increased to 15%. The increase in thermal conductivity with increasing fines content is expected to continue until the sand-silt granular mixture reaches the maximum dry mass density. The difference in the thermal conductivity of samples F00 and F15 was reduced 1.8 times after MICP treatment, compared to the initial saturated state. Results indicated that the effect of fines content on thermal conductivity can be reduced by increasing the number of pulses. The observed behavior was attributed to the reduction in porosity due to $CaCO_3$ precipitation.

The increased filtration effect due to reduced size of the pore throats in the presence of fine particles was found to have a negligible impact on the effect of bio-cementation on the thermal conductivity of the soil.

CHAPTER FOUR

CONCLUSION AND OUTLOOK

Conclusion

A series of column experiments were conducted to investigate the effect of fines content on bio-cementation process and thermal properties of bio-cemented silty sand. Ureolytic bacterium *Sporosarcina pasteurii* was used as a source of urease enzyme. The results were used to investigate the calcium carbonate precipitation profile and the evaluation of the thermal conductivity of MICP treated silty sand specimens (with fines contents of 0%, 5%, and 15%).

Two different injection strategies were tested in sand columns to investigate the effects of introducing the injection fluids from the bottom to top, and alternatively from the top and the bottom by flipping the specimen. The results showed more uniform distribution of cementation through the specimen length and higher amount of urea hydrolysis in the specimen treated with the alternating method. Injection rate was determined based on the experimental observations, a flow rate for efficient ureolytic activity was the selected for the specimen size and soil characteristics used in this study.

Five soil columns were subjected to MICP treatment with alternating injection method. All specimens displayed a similar cementation pattern within the columns with higher concentration at the injection port and lower concentration at the middle of the specimen. Measurements from effluent sampling and post-treatment acid digest methods showed a lower precipitation with increasing fines content. This was expected as the samples with higher silt content have lower pore volume and received lower amount of injection fluids. For all specimens, the amount of precipitated $CaCO_3$ gradually decreases as the distance from the top and bottom injection ports increases. This was attributed to the filtration of bacterial cells through the soil particles, resulting in a higher cementation near the injection points.

Measurements of thermal conductivity were obtained prior to and during MICP treatment. Thermal conductivity increased with the number of pulses for all specimens when compared to the control specimen. Under the saturated and untreated conditions, thermal conductivity increased by about 11% when fines content was increased to 15%. The increase in thermal conductivity with increasing fines content is expected to continue until the sand-silt granular mixture reaches the maximum dry mass density. The difference in the thermal conductivity of samples F00 and F15 was reduced 1.8 times after MICP treatment, compared to the initial saturated state. Results indicated that the effect of fines content on thermal conductivity can be reduced by increasing the number of pulses. The observed behavior was attributed to the increased solid mass in the soil matrix due to $CaCO_3$ precipitation. The increased filtration effect due to reduced size of the pore throats in the presence of fine particles (Zamani, 2017) was found to have a negligible impact on the effect of bio-cementation on the thermal conductivity of the soil.

Recommendations for Future Work

Research has shown that microbiological soil improvement methods have the potential to improve thermo-hydro-mechanical properties of geomaterials (Cheng et al., 2013; Martinez et al., 2019; Mujah et al., 2021; Venuleo et al., 2016). The application of microbial induced calcite precipitation on silty sands and its potential for an efficient improvement of the thermal properties soil on fine grain sand and silty sands is explored. The application of MICP can be extended through injection rate and distribution of the treatment media and the chemical recipes depending on the targeted soil improvement. Presence of silt adds complexity to the applicability of MICP soil improvement method due to the reduced permeability compared to clean sands. For the future work of this study, MICP treatment on the silty sand should be tested when the critical fines content is reached where the characteristics sand mixture starts to change. Additionally, different injection methods including using a spacer solution to achieve more homogenous distribution of cementation can be tested for the MICP applications in soils with fines content. Future studies should also include investigations of different injections strategies that are applicable in-situ. Further investigation is necessary to provide an insight to the efficiency of the improvement in thermal properties using MICP method for different types of soil.

REFERENCES CITED

Al Qabany, A., Soga, K., Santamarina, C. 2012. Factors Affecting Efficiency of Microbially Induced Calcite Precipitation. *Journal of Geotechnical and Geoenvironmental Engineering*, **138**(8), 992-1001.

Alrtimi, A., Rouainia, M., Haigh, S. 2016. Thermal conductivity of a sandy soil. *Applied Thermal Engineering*, **106**, 551-560.

Barkouki, T.H., Martinez, B.C., Mortensen, B.M., Weathers, T.S., De Jong, J.D., Ginn, T.R., Spycher, N.F., Smith, R.W., Fujita, Y. 2011. Forward and Inverse Bio-Geochemical Modeling of Microbially Induced Calcite Precipitation in Half-Meter Column Experiments. **90**.

Beziat, A., Dardaine, M., Mouche, E. 1992. Measurements of the thermal conductivity of clay-sand and clay-graphite mixtures used as engineered barriers for high-level radioactive waste disposal. *Applied clay science,* **6**(4), 245-263.

Brandl, H. 2006. Energy foundations and other thermo-active ground structures. *Géotechnique*, **56**(2), 81-122.

Cheng, L., Cord-Ruwisch, R., Shahin, M.A. 2013. Cementation of sand soil by microbially induced calcite precipitation at various degrees of saturation. *Canadian Geotechnical Journal*, **50**(1), 81-90.

Chou, C.-W., Seagren, E., Asce, A., Aydilek, A., Asce, M., Lai, M. 2011a. Biocalcification of Sand through Ureolysis. *Journal of Geotechnical and Geoenvironmental Engineering*, **137**.

Chou, C.-W., Seagren, E.A., Aydilek, A.H., Lai, M. 2011b. Biocalcification of sand through ureolysis. *Journal of Geotechnical and Geoenvironmental Engineering*, **137**(12), 1179-1189.

Cunningham, W.A., Zelazo, P.D., Packer, D.J., Van Bavel, J.J. 2007. The iterative reprocessing model: A multilevel framework for attitudes and evaluation. *Social Cognition*, **25**(5), 736-760.

Cuthbert, M.O., McMillan, L.A., Handley-Sidhu, S., Riley, M.S., Tobler, D.J., Phoenix, V.R. 2013. A field and modeling study of fractured rock permeability reduction using microbially induced calcite precipitation. *Environmental science & technology*, **47**(23), 13637-13643.

Dawoud, B., Amer, E.H., Gross, D.M. 2007. Experimental investigation of an adsorptive thermal energy storage. *International journal of energy research*, **31**(2), 135-147.

DeJong, J.T., Fritzges, M.B., Nüsslein, K. 2006. Microbially induced cementation to control sand response to undrained shear. *Journal of geotechnical and geoenvironmental engineering*, **132**(11), 1381-1392.

DeJong, J.T., Mortensen, B.M., Martinez, B.C., Nelson, D.C. 2010. Bio-mediated soil improvement. *Ecological Engineering*, **36**(2), 197-210.

Ebigbo, A., Phillips, A., Gerlach, R., Helmig, R., Cunningham, A.B., Class, H., Spangler, L.H. 2012a. Darcy-scale modeling of microbially induced carbonate mineral precipitation in sand columns. *Water Resources Research*, **48**(7).

Ebigbo, A., Phillips, A., Gerlach, R., Helmig, R., Cunningham, A.B., Class, H., Spangler, L.H. 2012b. Darcy-scale modeling of microbially induced carbonate mineral precipitation in sand columns. *Water Resources Research*, **48**(7).

Farouki, O.T. 1981. The thermal properties of soils in cold regions. *Cold Regions Science and Technology*, **5**(1), 67-75.

Feng, K., Montoya, B. 2015. Drained shear strength of MICP sand at varying cementation levels. in: *IFCEE 2015*, pp. 2242-2251.

Feng, K., Montoya, B.M. 2016. Influence of Confinement and Cementation Level on the Behavior of Microbial-Induced Calcite Precipitated Sands under Monotonic Drained Loading. *Journal of Geotechnical and Geoenvironmental Engineering*, **142**(1), 04015057.

Foppen, J.W., Schijven, J.F. 2006. Evaluation of data from the literature on the transport and survival of Escherichia coli and thermotolerant coliforms in aquifers under saturated conditions. *Water Res*, **40**(3), 401-26.

Ginn, T.R., Wood, B.D., Nelson, K.E., Scheibe, T.D., Murphy, E.M., Clement, T.P. 2002. Processes in microbial transport in the natural subsurface. *Advances in Water Resources*, **25**(8), 1017-1042.

Gomez, M.G., Anderson, C.M., Graddy, C.M.R., DeJong, J.T., Nelson, D.C., Ginn, T.R. 2017. Large-Scale Comparison of Bioaugmentation and Biostimulation Approaches for Biocementation of Sands. *Journal of Geotechnical and Geoenvironmental Engineering*, **143**(5), 04016124.

Gunyol, P., Khosravi, M., Phillips, A., Plymesser, K. 2022. Thermal Properties of Bio-Cemented Sand. in: *Geo-Congress 2022*, pp. 356-364.

Harkes, M.P., Van Paassen, L.A., Booster, J.L., Whiffin, V.S., van Loosdrecht, M.C. 2010. Fixation and distribution of bacterial activity in sand to induce carbonate precipitation for ground reinforcement. *Ecological Engineering*, **36**(2), 112-117.

Hommel, J., Akyel, A., Frieling, Z., Phillips, A., Gerlach, R., Cunningham, A., Class, H. 2020. A Numerical Model for Enzymatically Induced Calcium Carbonate Precipitation. *Applied Sciences*, **10**, 4538.

Hommel, J., Lauchnor, E., Phillips, A., Gerlach, R., Cunningham, A.B., Helmig, R., Ebigbo, A., Class, H. 2015. A revised model for microbially induced calcite precipitation: Improvements and new insights based on recent experiments. *Water Resources Research*, **51**(5), 3695-3715.

Ismail, A.F., Hassan, A.R., Cheer, N.B. 2002a. Effect of shear rate on the performance of nanofiltration membrane for water desalination. *Songklanakarin J. Sci. Technol*, **24**, 879-889.

Ismail, M., Joer, H.A., Randolph, M., Meritt, A. 2002b. Cementation of porous materials using calcite. *Geotechnique*, **52**, 313-324.

Jung, D., Biggs, H., Erikson, J., Ledyard, P.U. 1975. New colorimetric reaction for end-point, continuous-flow, and kinetic measurement of urea. *Clinical Chemistry*, **21**(8), 1136-1140.

Kirkland, C.M., Akyel, A., Hiebert, R., McCloskey, J., Kirksey, J., Cunningham, A.B., Gerlach, R., Spangler, L., Phillips, A.J. 2021. Ureolysis-induced calcium carbonate precipitation (UICP) in the presence of CO2-affected brine: A field demonstration. *International Journal of Greenhouse Gas Control*, **109**, 103391.

Likos, W.J. 2015. Pore-scale model for thermal conductivity of unsaturated sand. *Geotechnical and Geological Engineering*, **33**(2), 179-192.

Lin, H., Suleiman, M.T., Brown, D.G., Kavazanjian, E. 2016a. Mechanical Behavior of Sands Treated by Microbially Induced Carbonate Precipitation. *Journal of Geotechnical and Geoenvironmental Engineering*, **142**(2), 04015066.

Lin, H., Suleiman, M.T., Brown, D.G., Kavazanjian Jr, E. 2016b. Mechanical behavior of sands treated by microbially induced carbonate precipitation. *Journal of Geotechnical and Geoenvironmental Engineering*, **142**(2), 04015066.

Martinez, A., Huang, L., Gomez, M. 2020. Enhancement of the thermal conductivity of sands via microbially-induced calcite precipitation. *E3S Web of Conferences*, **205**, 09011.

Martinez, A., Huang, L., Gomez, M.G. 2019. Thermal conductivity of MICP-treated sands at varying degrees of saturation. *Géotechnique Letters*, **9**(1), 15-21.

Martinez, B.C., DeJong, J.T., Ginn, T.R., Montoya, B.M., Barkouki, T.H., Hunt, C., Tanyu, B., Major, D. 2013. Experimental Optimization of Microbial-Induced Carbonate Precipitation for Soil Improvement. *Journal of Geotechnical and Geoenvironmental Engineering*, **139**(4), 587-598.

McCartney, J.S., Sánchez, M., Tomac, I. 2016. Energy geotechnics: Advances in subsurface energy recovery, storage, exchange, and waste management. *Computers and Geotechnics*, **75**, 244-256.

Midttømme, K., Roaldset, E. 1998. The effect of grain size on thermal conductivity of quartz sands and silts. *Petroleum Geoscience*, **4**, 165-172.

Mitchell, A.C., Phillips, A., Schultz, L., Parks, S., Spangler, L., Cunningham, A.B., Gerlach, R. 2013. Microbial CaCO3 mineral formation and stability in an experimentally simulated high pressure saline aquifer with supercritical CO2. *International Journal of Greenhouse Gas Control*, **15**, 86-96.

Montoya, B., DeJong, J. 2015a. Stress-strain behavior of sands cemented by microbially induced calcite precipitation. *Journal of Geotechnical and Geoenvironmental Engineering*, **141**(6), 04015019.

Montoya, B.M. 2012. *Bio-mediated soil improvement and the effect of cementation on the behavior, improvement, and performance of sand*. University of California, Davis.

Montoya, B.M., DeJong, J.T. 2015b. Stress-Strain Behavior of Sands Cemented by Microbially Induced Calcite Precipitation. *Journal of Geotechnical and Geoenvironmental Engineering*, **141**(6), 04015019.

Mujah, D., Shahin, M.A., Cheng, L., Karrech, A. 2021. Experimental and Analytical Study on Geomechanical Behavior of Biocemented Sand. *International Journal of Geomechanics*, **21**(8), 04021126.

Phillips, A.J. 2013. Biofilm-induced calcium carbonate precipitation application in the subsurface, Bozeman, Montana : Montana State University. Bozeman, Montana.

Phillips, A.J., Cunningham, A.B., Gerlach, R., Hiebert, R., Hwang, C., Lomans, B.P., Westrich, J., Mantilla, C., Kirksey, J., Esposito, R. 2016. Fracture sealing with microbially-induced calcium carbonate precipitation: A field study. *Environmental science & technology*, **50**(7), 4111-4117.

Phillips, A.J., Gerlach, R., Lauchnor, E., Mitchell, A.C., Cunningham, A.B., Spangler, L. 2013. Engineered applications of ureolytic biomineralization: a review. *Biofouling*, **29**(6), 715-733.

Pouloupatis, P.D., Tassou, S.A., Christodoulides, P., Florides, G.A. 2017. Parametric analysis of the factors affecting the efficiency of ground heat exchangers and design application aspects in Cyprus. *Renewable Energy*, **103**, 721-728.

Rebata-Landa, V., Santamarina, J. 2006. Mechanical limits to microbial activity in deep sediments. *Geochemistry Geophysics Geosystems - GEOCHEM GEOPHYS GEOSYST*, **71**.

Rees, G., Friston, K., Koch, C. 2000. A direct quantitative relationship between the functional properties of human and macaque V5. *Nature neuroscience*, **3**(7), 716-723.

Sinyak, Y. 1994. Global climate and energy systems. *Science of the total environment*, **143**(1), 31-51.

Stocks-Fischer, S., Galinat, J.K., Bang, S.S. 1999. Microbiological precipitation of CaCO3. *Soil Biology and Biochemistry*, **31**(11), 1563-1571.

Tobler, D.J., Maclachlan, E., Phoenix, V.R. 2012. Microbially mediated plugging of porous media and the impact of differing injection strategies. *Ecological Engineering*, **42**, 270-278.

Van Paassen, L.A. 2009. Biogrout, ground improvement by microbial induced carbonate precipitation.

van Paassen, L.A., Ghose, R., van der Linden, T.J., van der Star, W.R., van Loosdrecht, M.C. 2010. Quantifying biomediated ground improvement by ureolysis: large-scale biogrout experiment. *Journal of geotechnical and geoenvironmental engineering*, **136**(12), 1721-1728.

Venuleo, S., Laloui, L., Terzis, D., Hueckel, T., Hassan, M. 2016. Microbially induced calcite precipitation effect on soil thermal conductivity. *Géotechnique letters*, **6**(1), 39-44.

Wang, Z., Zhang, N., Ding, J., Li, Q., Xu, J. 2020. Thermal conductivity of sands treated with microbially induced calcite precipitation (MICP) and model prediction. *International Journal of Heat and Mass Transfer*, **147**, 118899.

Whiffin, V.S. 2004. Microbial CaCO3 precipitation for the production of biocement, Murdoch University.

Whiffin, V.S., van Paassen, L.A., Harkes, M.P. 2007. Microbial Carbonate Precipitation as a Soil Improvement Technique. *Geomicrobiology Journal*, **24**(5), 417-423.

Xiao, Y., Tang, Y., Ma, G., McCartney, J.S., Chu, J. 2021. Thermal conductivity of biocemented graded sands. *Journal of Geotechnical and Geoenvironmental Engineering*, **147**(10), 04021106.

Yun, T., Santamarina, J. 2008. Fundamental study of thermal conduction in dry soils. *Granular Matter*, **10**, 197-207.

Zamani, A. 2017. Liquefaction Mitigation of Silty Sands with Microbial Induced Calcium Carbonate Precipitation.

Zamani, A., Montoya, B.M. 2018. Undrained Monotonic Shear Response of MICP-Treated Silty Sands. *Journal of Geotechnical and Geoenvironmental Engineering*, **144**(6), 04018029.

Zhang, N., Yu, X., Pradhan, A., Puppala, A.J. 2015. Effects of Particle Size and Fines Content on Thermal Conductivity of Quartz Sands. *Transportation Research Record*, **2510**(1), 36-43.

APPENDICES

APPENDIX A

SOIL INDEX TESTING

A dry sieve (ASTM D2488/D2487) and hydrometric analysis (ASTM D7928/D422) were used to separate particles into size ranges and determine the mass of particles in each range. Dry sieve analysis, performed in accordance with ASTM D2488/D2487, was conducted for the F-65 Ottawa sand. This test method uses a square-opening sieve criterion in determining the gradation of soil between the 3/8 in (9.53 mm) and No. 200 (0.075mm) sieves. The sieve analysis was repeated for two different 200g samples of Ottawa F-65 sand taken from a single batch. The results provided that the range of No. 60 (0.25 mm) to 100 (0.15 mm) held predominance over the material's particle size, each retaining over 15% of the soil. Fines (Sub-200) were negligible at 0.2% passing, so further analysis of the material was not deemed necessary. Loss was limited to 0.025% of the sample mass, minimally impacting results.

For the particle sizes smaller than 75-mm (2.95-in), the distribution of particles was determined by a sedimentation process, using a hydrometer. Hydrometric analysis tests were performed for the Si-Co-Sil 250. The hydrometer used was a type 151H, reporting out the specific gravity of the mixture at an effective depth. After thoroughly mixed, the solution's specific gravity was measured at 2, 4, 8, 16, and 30 minutes, then 1, 2, 4, 8, and 24 hours. Three additional measurements were collected after this final point in order to rectify some deficiencies in the data; the mixture was re-shaken for 1 minute, and allowed to settle again, measurements taken after 5, 30, and 60 seconds. Measurements taken at this initial period of settlement (from 0-60 seconds) accounted for the larger particle sizes not perceived by the 2-minute mark, as sedimentation is much more rapid. This helped to create a more contiguous curve, shown below (Fig. 2). The assumed value of specific gravity was 2.75 (Price, 2018).

APPENDIX B

ACID WASHING AND FLUID SAMPLING

Two approaches were used to evaluate the efficiency of calcium precipitation between the alternate injection methods: 1) acid washing, and 2) effluent sampling. In the first approach (acid washing), once cementation was complete and the specimen was dried, the PVC column was removed, and the remaining sand column was cut with a saw into 24 mm (0.94-in) pieces for evaluation of the treatment's homogeneity. Each section was crushed to powder using a grinder. One (1) gram of bio-cemented sand from each section was transferred into 15 mL centrifuge tubes with five (5) milliliters of Trace-metal-grade nitric acid (10%, Fisher Scientific) to dissolve the calcium carbonate (Figure 3). After the calcium carbonate was completely dissolved, the liquid was removed from the samples. The samples were placed in the oven at 45^{o} C until they were completely dried and the difference in the mass of the samples were measured in order to determine the amount of $CaCO_3$ dissolved in Trace-metal-grade nitric acid.

In the second approach (effluent sampling) a sample of effluent was collected in microcentrifuge tubes from the soil specimens after each batch period. Sixty (60) microliters of the effluent sample collected was transferred to five hundred and forty (540) microliters of 2M nitric acid (HNO_3) in order to stop the ongoing reaction in the effluent samples (Figure 3). Effluent samples were vortexed before and after the transfer. Further dilutions were performed using Trace-metal-grade nitric acid (5%) if necessary, in order to perform analyses for calcium concentration via colorimetric calcium assay and urea concentration via a modified colorimetric Jung assay (Jung et al., 1975; Phillips et al., 2013) .

APPENDIX C

CALCIUM AND UREA ASSAY DATA

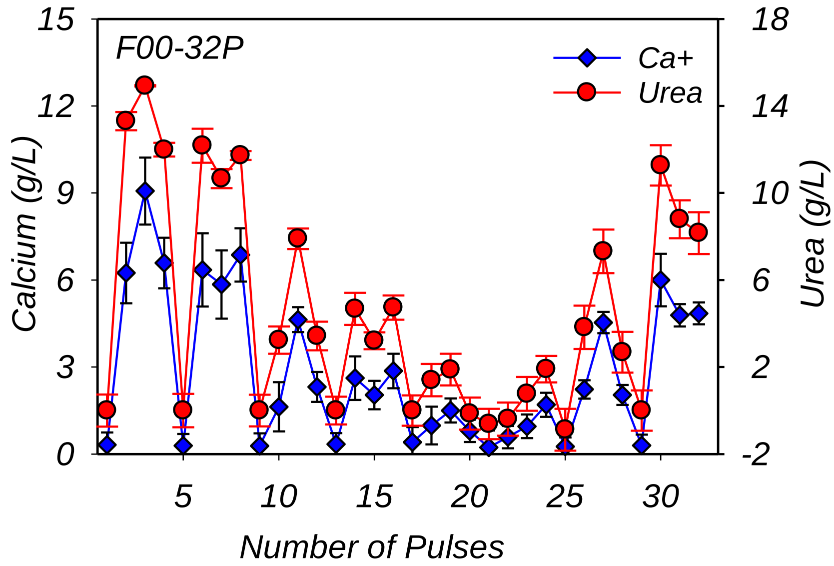

Figure C.1. Calcium Concentration and Urea Measurements from the Effluent Samples Specimens F00-P32

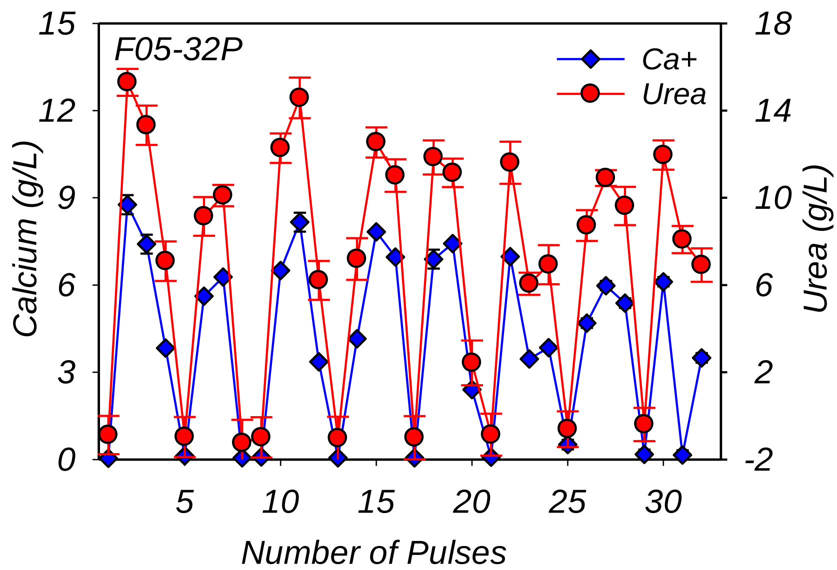

Figure C.2. Calcium Concentration and Urea Measurements from the Effluent Samples of Specimens F05-P32

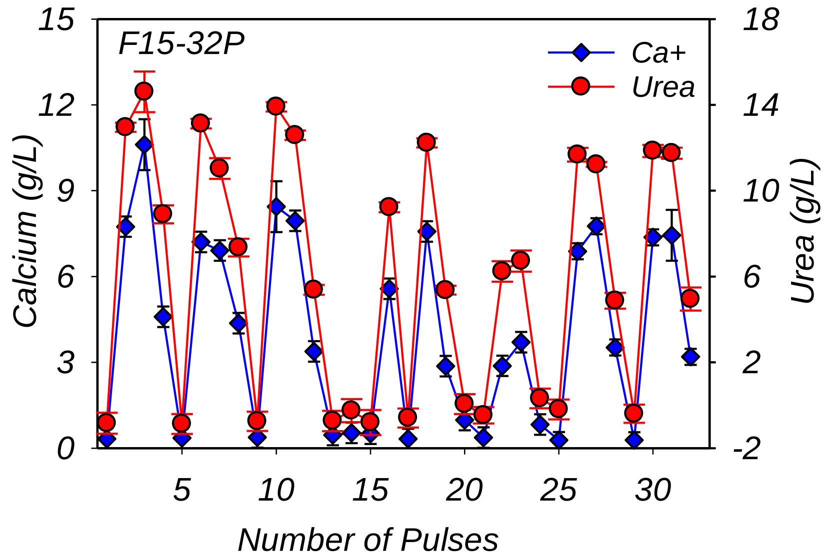

Figure C.3. Calcium Concentration and Urea Measurements from the Effluent Samples of Specimens F15-P32

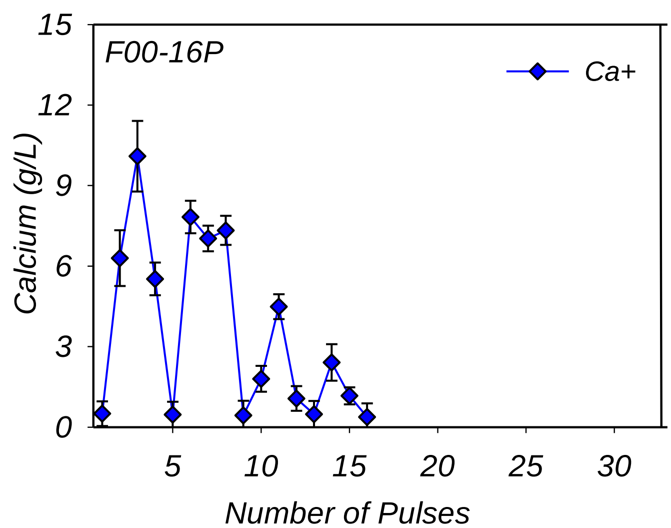

Figure C.4. Calcium Concentration Measurements from the Effluent Samples of Specimens F00-P32

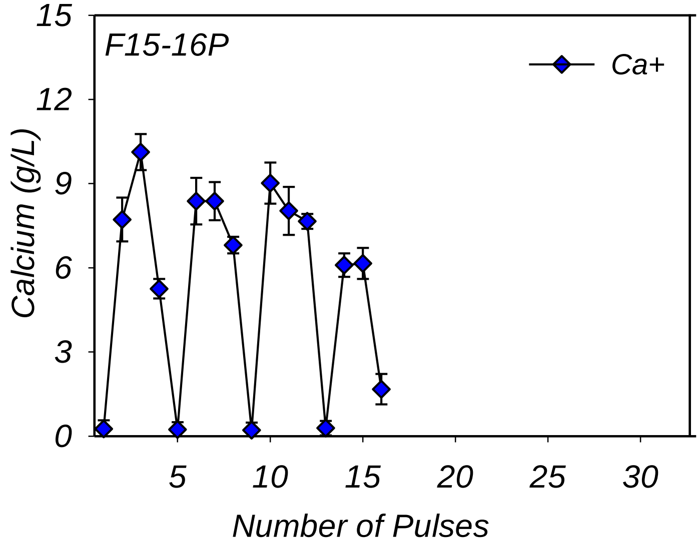

Figure C.5. Calcium Concentration Measurements from the Effluent Samples of Specimens F15-P32